Implications of hornbeam and beech root systems on slope stability: from field and laboratory measurements to modelling methods

Azade Deljouei[1,2]*, Alessio Cislaghi[3,4], Ehsan Abdi[5], Stelian Alexandru Borz[1], Baris Majnounian[5], Tristram C. Hales[6]

1. Department of Forest Engineering, Forest Management Planning and Terrestrial Measurements, Faculty of Silviculture and Forest Engineering, Transilvania University of Brasov, Şirul Beethoven 1, 500123 Brasov, Romania

2. School of Forest, Fisheries, and Geomatics Sciences, University of Florida, Gainesville, FL, USA

3. Department of Agricultural and Environmental Sciences, University of Milan, Milan, Italy

4. Centre of Applied Studies for the Sustainable Management and Protection of Mountain Areas (Ge.S.Di.Mont), University of Milan, Via Morino 8, Edolo, 25048 Brescia, Italy

5. Department of Forestry and Forest Economics, Faculty of Natural Resources, University of Tehran, Karaj, Iran

6. School of Earth and Environmental Sciences, Cardiff University, Cardiff, United Kingdom

*** Corresponding author: azade.deljouei@unitbv.ro or a.deljooei@ut.ac.ir (A. Deljouei)**

ORCID of the authors:

- Azade Deljouei: 0000-0003-3453-8530
- Alessio Cislaghi: 0000-0002-4618-818X
- Ehsan Abdi: 0000-0002-3382-7683
- Stelian Alexandru Borz: 0000-0003-4571-7235
- Tristram C. Hales: 0000-0002-3330-3302

Abstract

Purpose This study investigated root distribution and estimated root reinforcement by field and laboratory measurements and modelling methods, as a function of species, diameter at breast height (DBH), slope position, altitude, and vertical and horizontal distances from tree in Hyrcanian temperate ecoregion of Iran.
Method 1080 profile trenches with a maximum 1 m depth were excavated on upslope and downslope from trunks of *Carpinus betulus* and *Fagus orientalis* with DBH ranges of 7.5-32.5, 32.5-57.5, and 57.5-82.5 cm at three altitudes (400, 950, and 1300 m a.s.l.).
Results Root distribution results indicated that: (i) frequency of small roots (2-5 mm of diameter) of *C. betulus* and fine roots (0-2 mm) of *F. orientalis* are the highest, whereas the frequency of large roots (>10 mm) of both species is the lowest, (ii) the Root Area Ratio (RAR) of *C. betulus* is always higher than *F. orientalis*, (iii) the trees with larger DBH have a larger RAR than those with a smaller DBH, (iv) the RAR of *F. orientalis* is higher in upslope positions than in downslope ones; however, the RAR of *C. betulus* are similar in both positions, (v) RAR at 1300 m altitude is highest, and (vi) the RAR decreases with increasing distance from tree trunk and soil depth. Furthermore, it is shown that: (i) root reinforcement of *C. betulus* is higher than *F. orientalis*, (ii) altitude has a significant effect on root reinforcement of *C. betulus*, (iii) root reinforcement of large trees is the highest, and (iv) root reinforcement decreases with increasing distance from tree trunks.
Conclusion C. betulus is preferable to *F. orientalis* for increasing slope stability. Forest managers should consider this outcome when developing strategies for silvicultural treatment and reforestation projects in mountainous areas.

Keywords: Hillslope stabilization, Root mechanical properties, Root Bundle Model Weibull, Root distribution, Root reinforcement, Iran.

1. Introduction

Forests play a significant role in preventing and mitigating hydrogeomorphic hazards such as shallow landslides, rockfalls, and avalanches. Trees generally provide more protective functions than shrubs and herbs via higher rates of rainfall interception and transpiration (Sadeghi et al. 2020; Lin et al. 2020), greater soil coverage that reduces rain splash erosion potential (Lin et al. 2020; Williams et al. 2020), increased buttressing and arching (Gray and Sotir 1996), and greater soil reinforcement by roots (Morgan and Rickson 1995). Trees regulate catchment water balances through intercepting rainfall (Sadeghi et al. 2015; Panahandeh et al. 2022), altering hydraulic conductivity through the development of root conduits, and increasing transpiration rates (Stokes et al. 2014; Vergani et al. 2017a; Farahnak et al. 2019). Roots also physically reinforce the soil by adding tensile and compressive strength to the soil mantle. The additional strength reduces the potential for shallow landsliding as root penetrate the soil mantle and cross the failure planes (Norris et al. 2008). On hillslopes, thick roots can act as piles to reinforce the soil, while fine roots act in tension to strengthen the soil that acts as an apparent cohesion (Abdi et al. 2010a). Quantifying the mechanical effects of vegetation on hillslope stabilization remains an unsolved issue and has been investigated since 1960s (e.g., Endo and Tsuruta 1969; O'Loughlin 1974; Genet et al. 2008). Root systems stabilize the shallower soils along all of the edges

of potential failures that are often separated into reinforcement of the basal surface (which in shallow landslide systems is often the soil-bedrock interface), the sides of the failure via increasing the shear strength, and at the toe of the landslide via stiffening and buttressing under compression (Giadrossich et al. 2019). Lateral root reinforcement is the most effective mechanism in stabilizing landslide-prone slopes, with the contribution declining with increasing the landslide size (Milledge et al. 2014). Finally, the contribution of roots under compression consists in mobilizing an additional resistance across the shear plane, which leads to a complex bending-tensioning of rooted-soil (Schwarz et al. 2015).

The magnitude of root reinforcement depends on the root density (i.e. the number of roots into the soil), distribution with depth into the soil, root diameter, and root biomechanical properties (i.e., tensile resistance, elasticity, etc.) (Mao 2022). Within a forest setting, root reinforcement varies spatially as forest stand characteristics (such as tree spatial distribution), diameter at the breast height (DBH), tree age, tree species composition, distance from the trunk, topography, growth conditions (including soil temperature, soil depth, nutrient), and moisture content all vary (Genet et al. 2010; Hales and Miniat 2017; Cislaghi et al. 2021). It is the complexity of the spatial variability in root properties at a stand scale that makes modelling the lateral root distribution very challenging (Vergani et al. 2017a). In this regard, Root Area Ratio (RAR) is proposed as a robust index that can be derived from 2D surface observations for quantifying the presence of roots inside the soil (Bischetti et al. 2009; Mao et al. 2012; Arnone et al. 2016). However, even measuring this parameter requires significant field investigation via excavation pits. Without high spatial coverage, most excavation pits are dominated by fine roots (<2 mm) hence we have less information on coarse roots, especially roots larger than 10 mm (Giadrossich et al. 2020). Few studies measure root distributions as a function of DBH and distance from the tree trunk (Schwarz et al. 2010; Cislaghi et al. 2021).

Accurate slope stability analyses require observations of biomechanical properties and root distributions at different spatial scales and for different species (Ekanayake and Phillips 1999). Root reinforcement is usually applied as an apparent cohesion term in slope stability analyses. The magnitude of root reinforcement was first calculated using the pioneering Wu and Waldron (W&W) method based on the assumption that roots are elastic fibers extending perpendicular to a shear surface, moreover all roots break at the same time (Wu, 1976; Waldron, 1977). Pollen and Simon (2005) developed the Fiber Bundle Model (FBM) to address the apparent overestimation of root reinforcement by the W&W model. The FBM assumes a parallel root system with roots having similar elastic properties. When each root breaks, the load is continuously redistributed over the remaining roots until the entire bundle is broken. The Root Bundle Model Weibull (RBMw) estimates root reinforcement by calculating root distributions as a function of the observed root distribution at hillslope scales (Schwarz et al. 2013). RBMw has been used in different environments across the world, including temperate forests of Norway spruce (*Picea abies* (L.) H. Karst.; Schwarz et al. 2013, 2015; Vergani et al. 2014; Moos et al. 2016; Cohen and Schwarz 2017; Cislaghi et al. 2021), Jolcham oak (*Quercus serrate* Murray; Yamase et al. 2021), Monterey pine (*Pinus radiate* D. Don; Giadrossich et al. 2020), black locust (*Robinia pseudoacacia* L.; Zydroń et al. 2019; Zydroń and Gruchot 2021), black poplar (*Populus nigra* L.; Zydroń et al. 2019), common hornbeam (*Carpinus betulus* L.; Zydroń and Gruchot 2021), green alder (*Alnus viridis* (Chaix) D.C.), red willow (*Salix purpurea* L.), goat willow (*Salix caprea* L.), hazel (*Corylus avellana* L.), European ash (*Fraxinus excelsior* L.), and European larch (*Larix decidua* Mill.; Bischetti et al. 2007), silver birch (*Betula pendula* Roth.),

small-leaved lime (*Tilia cordata* Mill.), English oak (*Quercus robur* L.), and sweet cherry (*Prunus avium* L.; Zydroń and Gruchot 2021), sweet chestnut (*Castanea sativa* Mill.; Dazio et al. 2018; Cislaghi et al. 2021), European beech (*Fagus sylvatica* L.; Gehring et al. 2019; Cislaghi et al. 2021), Scots pine (*Pinus sylvestris* L.; Vergani et al. 2017b), and subtropical forest for the white mangrove (*Avicennia marina* (Forssk.) Vierh.; Karimi et al. 2022).

Given the complexity of estimating subsurface root parameters and the level of parameterisation required to develop effective root reinforcement models, we do not have methods for estimating root reinforcement at the hillslope scale. Biome-level estimates of root reinforcement can constrain root reinforcement to an order of magnitude (Hales 2018). Hillslope scale analysis of root reinforcement, such as mapping diameter at breast height (Roering et al. 2003), still requires high levels of field validation. Field validation is particularly important in landslide prone but data poor locations such as the Hyrcanian temperate forests. In these forests, few studies provided useful advances for implementing nature-based solutions such as the forests, to reduce the negative impacts of shallow landslides. Abdi et al. (2010a) observed that RAR of oriental beech (*Fagus orientalis* Lipsky.), Persian ironwood (*Parrotia persica* (DC.) C.A.Mey.) and *Carpinus betulus* trees decreased with the depth and the maximum RAR values in the upper soil layers. For three pioneer species, Caucasian alder (*Alnus subcordata* C.A.Mey), velvet maple (*Acer velutinum* Boiss.), and Persian ironwood, Abdi and Deljouei (2019) showed that RAR was higher in shallower depths of the soil and in profiles nearer trees, they showed significantly higher RAR than in far trenches. Deljouei et al. (2020) explored the most important parameters that affect fine roots resistance of two common temperate species (*F. orientalis* and *C. betulus*) in the Hyrcanian forest, finding that tree species and DBH make a significant difference in fine roots resistance. The complexity of the subsurface pattern of soil profiles, tree DBH, altitude, and slope positions and their effects on the spatial variability of roots and root reinforcement is still underexplored (Hales et al. 2009; Moos et al. 2016; Hales and Miniat 2017; Cislaghi et al. 2021). For these reasons, the present study focuses on spatial and mechanical characteristics of the root systems of the dominant species (*F. orientalis* and *C. betulus*) in the Hyrcanian forest. In such environment, *F. orientalis* forests account for approximately 30% of the standing volume and 23.6% of the stem number at altitudes from 300 to 2000 m a.s.l (Sagheb-Talebi et al. 2014). Meanwhile, *C. betulus* species accounts for 30.5% of the standing volume and 30% of the stem number and can be found at altitudes from 100 to 1500 m a.s.l (Sagheb-Talebi et al. 2014). Both species have extensive ranges in the mountains of Europe and Western Asia and occupy a wide elevation range that means they often occur on mountain slopes where the protection function of forests is important to reduce landslide risk to life and infrastructure.

Forestry decision-making is increasingly recognising the role of trees as a nature-based solution for protection, as well as the more traditionally recognised ecological and economic benefits. While a lot of work on root reinforcement has occurred in traditional European and North American forestry species (e.g. Douglas fir and Sitka spruce), a systematic understanding of the variability in root reinforcement of common non-forestry species is rarer in the literature. Hence we sought to understand how different environmental and topographic controls in two common species, *C. betulus* and *F. orientalis*. The main aims of the study were: (i) investigating the spatial (root distribution) and mechanical variability of root systems, and (ii) modelling root reinforcement by Root Bundle Model Weibull (RBMw) of two hardwood species in the Hyrcanian forest; (iii) providing a simplified framework for evaluating the effects of trees in terms of slope stability. In addition, the study conducted a statistical analysis of the similarities and differences between two

main species of Hyrcanian temperate forests and several dendrometric characteristics, altitude, and spatial position on root reinforcement, which forest managers must consider to mitigate shallow landslides.

2. Material and Methods

2.1. Study site

Iran a landslide-prone country due to its specific geologic, morphologic, climatic, and tectonic conditions. Approximately 2600 landslides occurred in the year 2000 in the country, which caused 162 deaths, destruction of 176 houses, and damages to 170 roads, with most landslides are concentrated on the rim of the Alborz Mountains in the Hyrcanian ecoregion (Abbaszadeh Shahri and Maghsoudi 2021). Hyrcanian forests are classified as hilly and mountainous temperate forests, forming a green belt over the northern slopes of the Alborz Mountain, with landslides often triggered where these areas have been cleared to construct roads. The forests cover ~1.9 million hectares of the southern coast of the Caspian Sea. The area is abundant in hardwood species, including approximately 50 trees and 80 shrub species (Fathizadeh et al. 2020; Rahbarisisakht et al. 2021). Dominant species are the *Carpinus betulus*, *Fagus orientalis*, *Parrotia persica*, Cappadocian maple (*Acer cappadocicum* Gled.), *Acer velutinum*, common alder (*Alnus glutinosa* (L.) Gaertn), Wych elm (*Ulmus glabra* Huds.), and the chestnut-leaved oak (*Quercus castaneifolia* C.A.Mey.). Hyrcanian forests are used for wood production, tourism, environmental protection and supportive services, such as soil conservation and maintenance of water resources (Heshmatol Vaezin et al. 2022; Panahandeh et al. 2022). One of the severe problems in Hyrcanian forests is slope failure and shallow landslides, specifically where the trees have been clear-cut to make space for forest roads (Abdi et al. 2010a). In this ecoregion, landslides often cause economic losses, property damages and high maintenance costs, as well as injuries or mortality (Pourghasemi et al. 2012).

Kheyrud Forest, which covers an area of ~8000 ha, was selected as the study location (Fig. 1). The climate of the area is humid, and the temperature fluctuations are relatively limited. The average annual precipitation is 1300 mm, falling mainly as rain. The mean summer and winter temperatures are estimated to be 25.1 and 7.1 °C, respectively (Haghshenas et al. 2016). Field sampling was carried out in three districts of the Kheyrud Forest (Fig. 1), namely Patom (latitudes 36° 35′ 59″ to 36° 36′ 9″ N and longitudes 51° 33′ 43″ to 51° 33′ 55″ E), Namkhane (latitudes 36° 33′ 45″ to 36° 33′ 55″ N and longitudes 51° 35′ 51″ to 51° 36′ 4″ E), and Chelir (latitudes 36° 32′ 45″ to 36° 32′ 55″ N and longitudes 51° 39′ 53″ to 51° 40′ 5″ E). Altitude of the study sites ranges from 400 m a.s.l. in Patom, with the highest mean temperature and lowest annual precipitation, to 950 m a.s.l. in Namkhane, and 1300 m a.s.l. in Chelir, the latter exhibiting the lowest mean temperature and the highest yearly precipitation. According to the unified soil classification system, the soils on the three study sites were clays with high plasticity (i.e., CH). The mean values (± SD) of the Atterberg limits of the soils (soil liquid limit (Casagrande cup method), soil plastic limit (rolling and thread method), and soil plasticity index) from the study sites were estimated at 65% (± 6.2%), 26.4% (± 3.1%), 38.6% (± 3.8%) in Patom district, 88.5% (± 7.4%), 38.3% (± 4.9%), 50.2% (± 4.6%) in Namkhane district, and 85.7% (± 6.9%), 37.7% (± 3.7%), 48.0% (± 5.0%) in Chelir district, respectively.

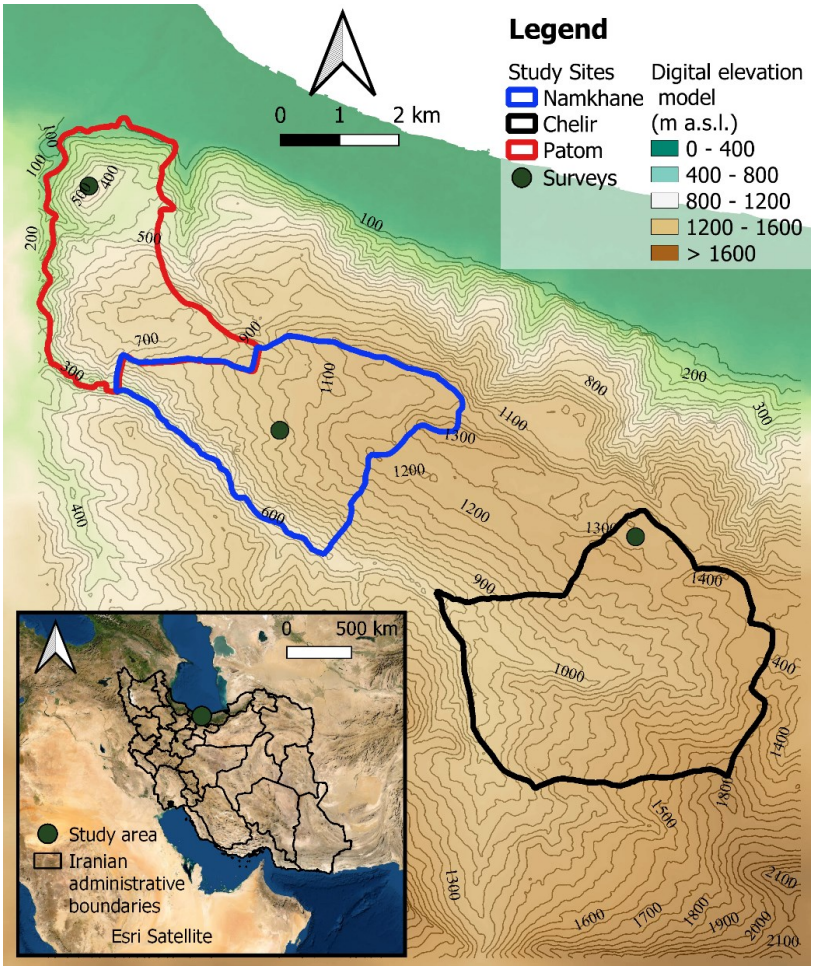

Fig. 1 Study location: map of Iran showing the general location of the study and districts taken into study

2.2. Measuring root distribution

Root distribution was measured for 5 sample trees of each of the two investigated species (*C. betulus* and *F. orientalis*), for each study site (Patom, Namkhane, and Chelir) at an altitude of 400, 950, and 1300 m a.s.l., respectively, and for each DBH class (small = 7.5-32.5 cm, medium = 32.5-57.5 cm, and large = 57.5-82.5 cm). Hence, 90 trees were randomly selected (3 altitudes × 3 DBH classes × 2 species × 5 trees) and used as a sampling reference in this study. Six trenches with a width of 0.5 m and a length of 1 m were excavated manually to the maximum rooting depth (1 m soil depth); located on the downslope and upslope at distances of 1.0 m, 1.5 m, 2.0 m, 2.5 m, 3.5 m, and 4.0 m from the tree (Fig. S1). The profile trenching method was used to characterize the root distribution (Böhm 1979; Fig. S1). Layers of 10 cm were marked on the vertical profile walls using pins and string (Fig. S1). The number of roots, diameter, and maximum depth were measured in both downslope and upslope trenches. The diameters of roots intersecting the soil profile were measured with a digital calliper. Based on their diameter, the roots were included in four classes, namely fine roots (0-2 mm), small roots (2-5 mm), medium roots (5-10 mm), and large roots (>10 mm).

The field measurements were conducted between August and October 2016. All the steps of collecting data are shown in Fig. 2.

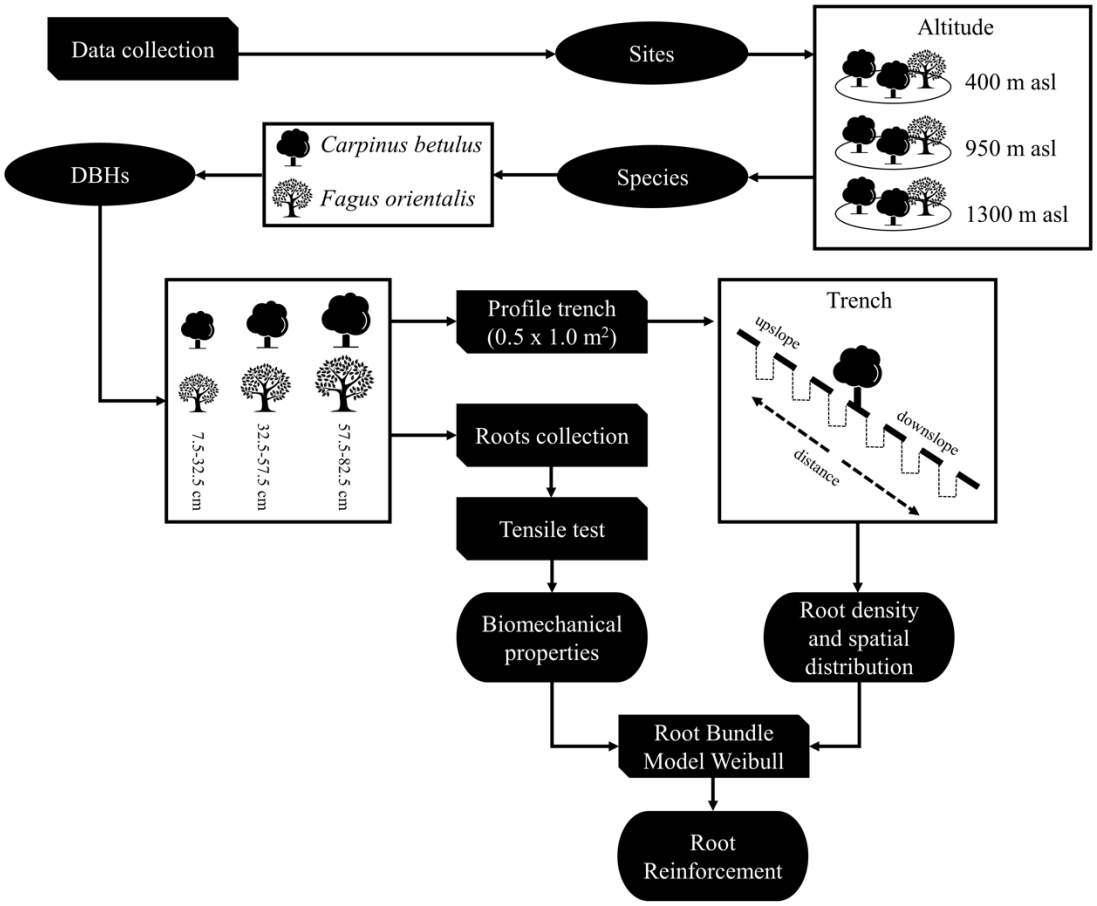

Fig. 2 Flowchart describing the steps for quantifying root reinforcement: selecting study sites at different altitudes (400 m a.s.l., 950 m a.s.l., 1300 m a.s.l.), selecting *Carpinus betulus* and *Fagus orientalis* samples with different DBH classes (small: 7.5-32.5 cm, medium: 32.5-57.5 cm, large: 57.5-82.5 cm), evaluating root density and spatial distribution at downslope and upslope at six distances from a tree trunk (1, 1.5, 2, 2.5, 3.5, and 4 m), investigating roots biomechanical properties and quantifying root reinforcement by Root Bundle Model Weibull

2.3. Measuring biomechanical properties

Root samples were collected from downslope and upslope at a depth of about 30 cm from the surface (Mao et al. 2012). To prevent mould and microbial degradation, a 15% alcohol solution was sprayed on the roots, then the treated roots were placed into plastic bags and refrigerated (4 °C) until tested (time between sampling and testing in the laboratory was of about 48 h) (Vergani et al. 2012). Roots with a length of 15 cm were placed in the clamps of the Universal Testing Machine (SANTAM Co./SMT-5, Tehran, Iran), and mechanical tests were conducted at a speed of 10 mm min^{-1} until rupture occurred. Only specimens that broke near the middle of the root segment were considered. Then, the relationships between the root diameter and biomechanical properties (i.e., maximum tensile force, Young's modulus, maximum elongation) were calculated using the following equations,

$$F_{\max}(\phi_i) = F_0\left(\frac{\phi_i}{\phi_0}\right)^{\xi} \quad (1)$$

$$E(\phi_i) = E_0\left(\frac{\phi_i}{\phi_0}\right)^{\beta} \quad (2)$$

$$L(\phi_i) = L_0\left(\frac{\phi_i}{\phi_0}\right)^{\alpha} \quad (3)$$

where ϕ_i is root diameter (in mm), ϕ_0 is the reference root diameter (1 mm), F_{max} is maximum tensile force (in N), E is root elasticity (MPa), and L is root elongation (in mm). F_0, E_0, and L_0 are multiplicative coefficients (in N, MPa, and mm, respectively), ξ, β, and α are exponential parameters (unitless).

2.4. Root Bundle Model Weibull (RBMw)

Root reinforcement was calculated using the Root Bundle Model Weibull (RBMw; Schwarz et al. 2013). RBMw is a strain-step fiber bundle model, developed to include the failure probability of roots due to variability in root mechanical properties. RBMw calculates force-displacement behaviour of a root bundle based on root distribution in diameter classes and on a series of power-distributed relationships (Eqs. 1-3). Root reinforcement c_r (in kPa) is calculated by summing up the force contributions F (in N) for each root per unit of area (m^2) multiplied by the Weibull survival function S (unitless), as follows:

$$c_r = \sum_{i=1}^{N} F(\phi_i, \Delta x) S(\Delta x^*) \quad (4)$$

Where Δx is the displacement unit in mm and S is a function of the normalized displacement Δx^* (unitless). The following equation calculates the $S(\Delta x^*)$:

$$S(\Delta x^*) = \exp\left[-\left(\frac{\Delta x^*}{\lambda}\right)^{\omega}\right] \quad (5)$$

In equation (5), λ is the scale Weibull parameter (unitless) and ω is the shape Weibull parameter (unitless).

The ratio between the displacements is estimated by each single tensile tests and the corresponding displacement values are calculated using fitted values of tensile forces.

$$F(\phi_i, \Delta x) = \frac{\pi E_0}{4 L_0}\phi_i^{\,2+\beta-\alpha} \qquad F(\phi_i, \Delta x) < F_{max}(\phi_i) \quad (6)$$

All input parameters (F_0, E_0, L_0, ξ, β, and α) were calculated from the tensile tests.

2.5. Evaluation of hillslope stability using a probabilistic multidimensional approach

For assessing the effects of the implications of different forest coverage on slope stability, the present study adopted the model PRIMULA (PRobabilistIc MUltidimensional shallow Landslide Analysis), developed by Cislaghi et al. (2017) and based on three pioneering model MD-STAB (Multidimensional Shallow Landslide Model) implemented by Milledge et al. (2014). The model consists in a combination between a 3D limit equilibrium model and a Monte Carlo Simulation (MCS). It is based on several assumptions: (i) the force balance is applied to the center of a potential parallelepiped landsliding block, (ii) groundwater level is steady and parallel to the slope surface, (iii) infiltration, suction and capillary rise are not taken into consideration, and (iv) the single block is divided into saturated and unsaturated zones. PRIMULA includes earth pressure lateral forces, soil cohesion and basal-lateral root reinforcement acting on potential landslide boundaries. The Factor of Safety (*FoS*) can be estimated as the ratio between the resisting and the driving forces as follows:

$$FoS = \frac{F_{rb} + 2F_{rl} + F_{rd} + F_{ru} - F_{du}}{F_{dc}} \quad (7)$$

where F_{dc} is the downslope component of the central block weight, F_{du} is the active earth force acting on the central block from the upslope edge, F_{rd} is the passive earth force acting on the central block from the downslope edge, F_{rb} is the resisting basal force acting on the basal soil-bedrock boundary, F_{rl} is the resisting shear force acting on the two parallel slope sides of the block, F_{ru} is the lateral root reinforcement acting on the upslope side of the block. The unit of measure of all forces is N. A comprehensive description of all equations describing each component of Eq. 7 is reported in Appendix A, whereas more details are in Cislaghi et al. (2017).

Including the MCS into a slope stability analysis is an effective method for dealing with the uncertainty/variability of each input parameter by sampling from independent and random sets of possible values for each one to determine the distribution of *FoS*. In the present study, θ varies from 20° to 60°, γ_s is normally distributed around 13.5 kNm^{-3} (Abdi and Deljouei 2019), φ' is uniformly distributed between 26° and 35°, C_s' is normally set around the average value of 15.3 kPa (Abdi and Deljouei 2019), and q_0 is in function of DBH class: 140 Nm^{-2}, 220 Nm^{-2}, and 320 Nm^{-2} for small, medium and large *C. betulus* trees, and 100 Nm^{-2}, 230 Nm^{-2}, and 400 Nm^{-2} for *F. orientalis* (Chiaradia et al. 2016; Hayati et al. 2017). The root reinforcement values of C_{rl}' are obtained by RBMw-calculations in the function of the most critical conditions i.e., distance from tree at 4 m by sampling and upslope position. C_{rb}' *i*s a percentage of C_{rl}' in the function of RAR and soil depth which depends on slip failure. The size of potential landslides is extracted by the statistical analysis conducted by Milledge et al. (2014) on six published worldwide landslide inventories. To summarize, the input parameters of PRIMULA are reported in Table 1. For this analysis, the procedure is replicated 1000 times; furthermore, to reduce the effects of random selection (Hammond et al. 1992).

Table 1. The parameters for PRIMULA in the function of species, altitude and DBH classes, considering the upslope position and the far distance from the trunk (i.e., 4 m). The parameters were specified using a range and the distribution function.

Parameter	Unit	Range	Distribution function	Reference
l/w	-	μ=1.42 σ=0.20	Normal	Milledge et al. 2014
D	m	[0.5; 1.5]	Uniform	Hammond et al. 1992
D_w/D	-	μ=0.80 σ=0.05	Normal	Schwarz et al. 2010
γ_s	kN m^{-3}	μ=13.5 σ=1.00	Normal	Abdi and Deljouei 2019
φ'	°	[26; 35]	Uniform	Abdi and Deljouei 2019
$\boldsymbol{C_s'}$	kPa	μ=15.3 σ=2.00	Normal	Abdi and Deljouei 2019

2.6. Statistical analysis

Statistical analysis was used to check the differences in root distribution and root reinforcement by considering the species, DBH, slope position, altitude, and distance from the trees. The Shapiro–Wilk and Levene's tests were used to check the normality and homogeneity of the data, respectively. Since the datasets were found to violate the normality and homogeneity assumptions, a nonparametric Kruskal-Wallis test (H) was used to compare the RAR and soil reinforcement of different root diameter classes within DBH classes, slope positions, and study sites for *C. betulus* and *F. orientalis* trees (Tables S1-S5). When the residuals were normal and variance was heterogeneous, parametric Welch t-tests were used to compare between two independent groups. Finally, when the residuals were normal and variance was homogenous, One-way ANOVA (analysis of variance) was used to compare the means of two or more groups for one dependent variable. All statistical analyses were implemented using the R software (https://www.r-project.org). Confidence intervals were set for a probability level of 0.05.

3. Results

3.1. Variability of root distribution

3.1.1. Root distribution as a function of species

RAR was measured by considering a number of 1080 profile trenches. Figure 3 showed the total RAR for fine (0-2 mm), small (2-5 mm), medium (5-10 mm), and large roots (>10 mm) as a function of species. Root distributions were remarkably different in regard to the diameter classes. As a fact, for *C. betulus*, small roots had the highest RAR value whereas the value of large roots was the lowest among all the root diameter classes (Fig. 3). Furthermore, fine roots of *F. orientalis* had a higher frequency compared with that from the rest of diameter classes (Fig. 3). The Kruskal-Wallis test indicated that RAR values of *C. betulus* was significantly higher than those of *F. orientalis* (H_1 = 65.13, H_1 = 140.65, H_1 = 177.01, H_1 = 117.44; p< 2.2e-16 to p<1e-15; for fine, small, medium, and large roots, respectively; Fig. 3 and Table S2). The total RAR (H_1 = 191.37, p< 2.2e-16; Fig. 4 and Table S2) and total roots per unit area (H_1 = 99.60, p< 2.2e-16; Fig. 4 and Table S2) of *C. betulus* and *F. orientalis* demonstrated a significant difference, in which *F. orientalis* had fewer roots. The minimum, maximum and mean values of RAR for *C. betulus* were 0.0010%, 0.0040%, and 0.0020%, respectively, while for *F. orientalis* the same statistics accounted for 0.0005%, 0.0020%, and

0.0010%, respectively. The results showed that *C. betulus* had more roots in all root diameter classes, in which the total number of roots per unit area for *C. betulus* was 38987 and for *F. orientalis* was 26079 (Fig. 4).

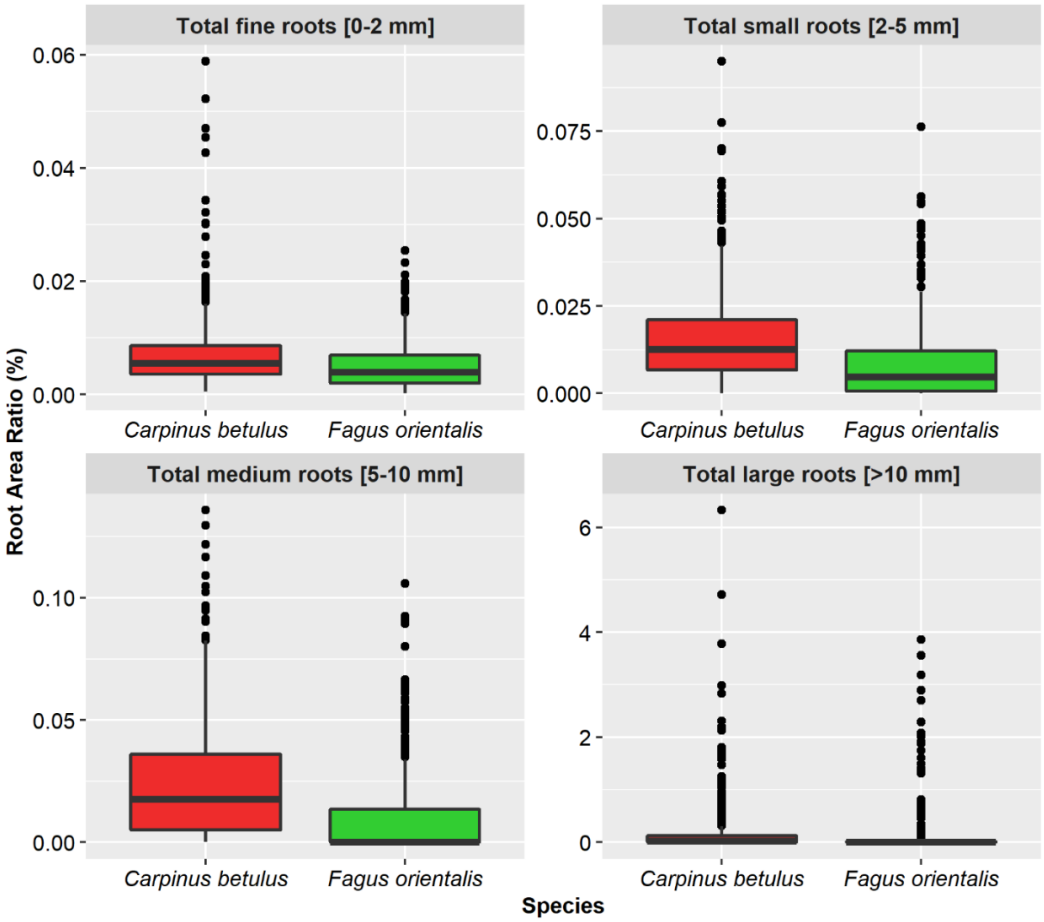

Fig. 3 Root Area Ratio (RAR, in %) of fine roots (0-2 mm), small roots (2-5 mm), medium roots (5-10 mm), and large roots (> 10 mm) as a function of species: *Carpinus betulus* and *Fagus orientalis*

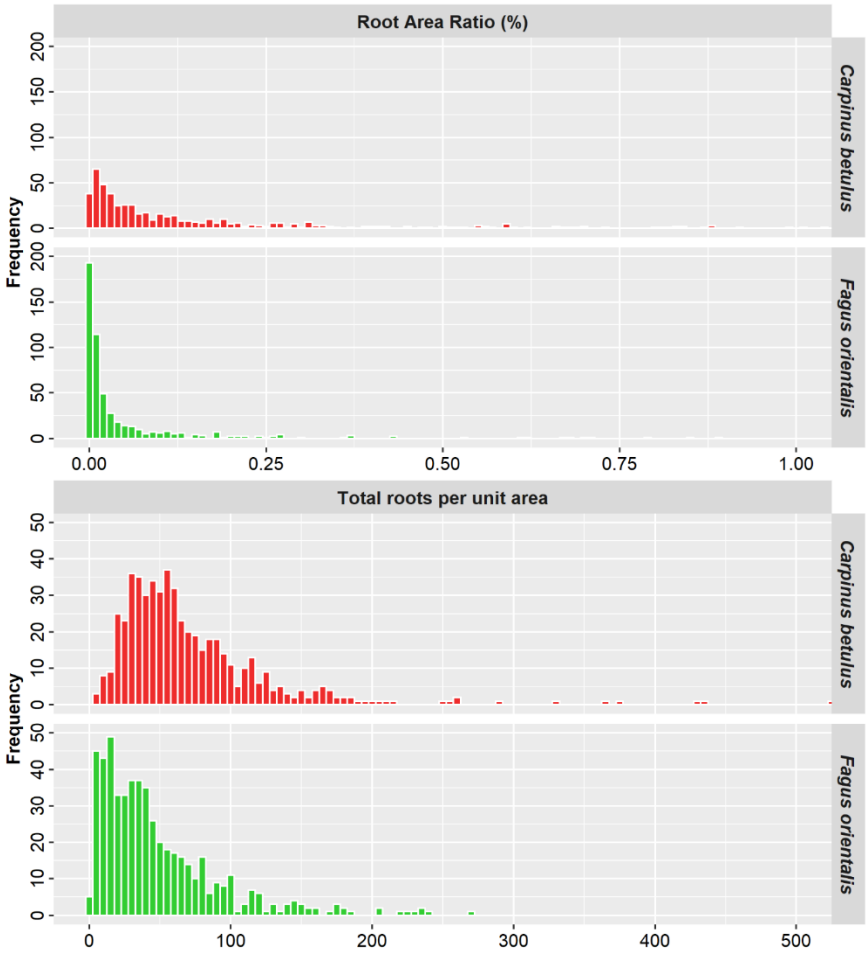

Fig. 4 Total Root Area Ratio (RAR, in %) and total roots per unit area as a function of tree species: *Carpinus betulus* and *Fagus orientalis*

3.1.2. Root distribution as a function of DBH

Kruskal-Wallis test was conducted to verify the differences in RAR as a function of DBH for *C. betulus* ($H_2 = 111.01$) and *F. orientalis* ($H_2 = 112.80$), in which significant differences were found to be caused by DBH classes of both species ($p < 2.2e\text{-}16$; Table S3). On average, the largest DBH tree class of both species had the highest RAR value compared to the other DBH classes (Fig. 5). The mean values of RAR for large trees was 0.0050% and 0.0030%, for *C. betulus* and *F. orientalis*, respectively (Fig. 5). Mean values of RAR for medium and small trees of *C. betulus* and *F. orientalis* were of 0.0010% and 0.0004%, 0.0006% and 0.0001%, respectively (Fig. 5).

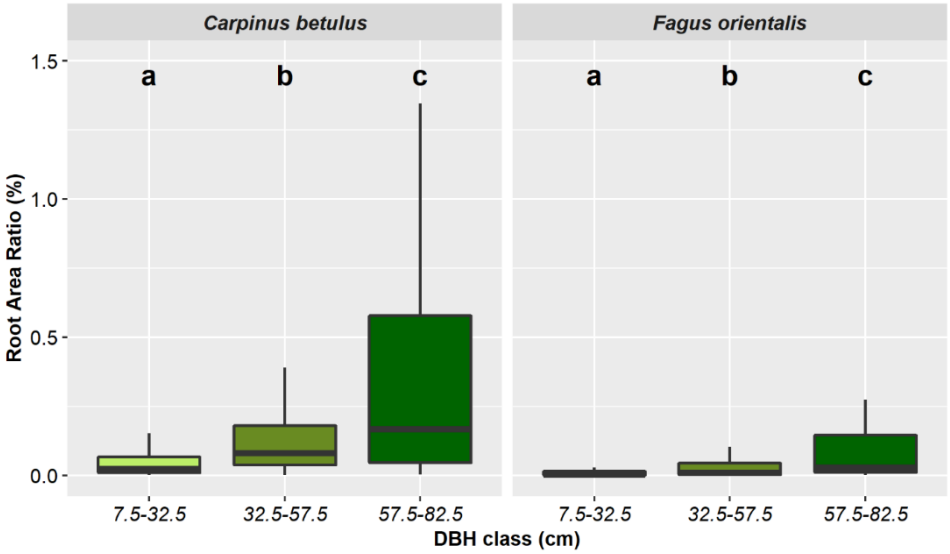

285

286 **Fig. 5** Root Area Ratio (RAR in %) for *Carpinus betulus* and *Fagus orientalis* as a function of DBH class: Small (7.5-
287 32.5 cm), Medium (32.5-57.5 cm), and Large (57.5-82.5 cm). Boxes with the similar lowercase letters are not
288 significantly different

289 **3.1.3. Root distribution as a function of slope position**

290 A synthesis of the RAR as a function of slope position is shown in Figure 5. RAR values of downslope and upslope
291 were not significantly different for *C. betulus* ($H_1 = 2.86$, $p = 0.09$; Table S4). However, while the RAR values of *F.*
292 *orientalis* were significantly higher for downslope ($H_1 = 7.01$, $p = 0.01$; Table S4). The mean value of RAR for
293 downslope and upslope of *C. betulus* was estimated to be 0.0020%, while the mean value of RAR for *F. orientalis* was
294 of 0.0020% and 0.0007% for downslope and upslope, respectively (Fig. 6).

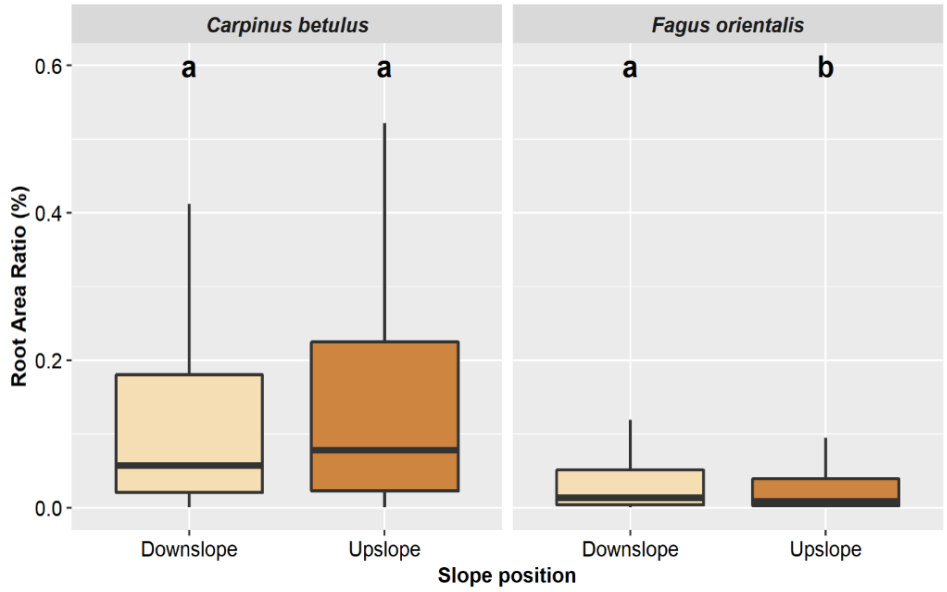

295

Fig. 6 Root Area Ratio (RAR in %) for *Carpinus betulus* and *Fagus orientalis* in function of slope position: Downslope and Upslope. Boxes with the similar lowercase letters are not significantly different

3.1.4. Root distribution as a function of altitude

Before proceeding with the statistical analysis on root distribution, we verified the assumption that the soil properties (and as consequence the root growth condition) of the three study sites (Patom, Namkhane, and Chelir at an altitude of 400, 950, and 1300 m a.s.l., respectively) were similar. Applying ANOVA, the soil samples showed no significant differences among the study sites (liquid limit: F= 4.13, p> 0.01; plastic limit: F= 4.76, p> 0.01; and plasticity index: F= 1.91, p> 0.01). Concerning RAR, the values varied among altitudes: 400, 950, and 1300 m of *C. betulus* (H_2 = 32.73, p<1e-7; Table S5) and *F. orientalis* (H_2 = 6.46, p=0.04; Table S5). Figure 7 showed the statistical differences brought by the altitude on the RAR of the two species. For *C. betulus*, the highest mean value of RAR was found in 1300 m (0.0020%) and it was followed by 950 m (0.0010%) and 400 m (0.0030%). For *F. orientalis*, RAR values in 1300 and 950 m were larger than in 400 m (Fig. 7). According to the altitude, mean RAR for *F. orientalis* was reported as 0.0010% for 1300 m and 950 m; furthermore, it was recorded as 0.0009% for 400 m (Fig. 7).

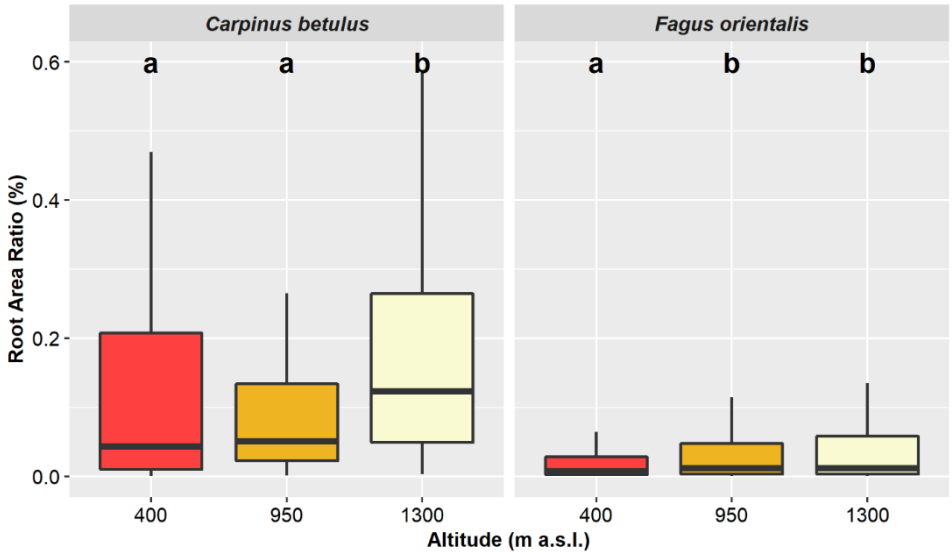

Fig. 7 Root Area Ratio (RAR in %) for *Carpinus betulus* and *Fagus orientalis* as a function of altitude: 400, 950, and 1300 m a.s.l. Boxes with the similar lowercase letters are not significantly different

3.1.5. Root distribution as a function of vertical and horizontal directions

In the case of both species, the predominant number of roots was found in the subsurface soil layers to a depth of up to 30 cm after which the root frequency decreased (Fig. 8). For both *C. betulus* and *F. orientalis*, RAR decreased monotonically with distance to tree beyond a 2 m (Fig. 8). The highest RAR values were found closest to the tree trunk with greater concentrations at 1-1.5 m from the tree trunk for both species (Fig. 8). The mean RAR at 1 m distance was calculated 0.07% and 0.06% for *C. betulus* and *F. orientalis*, respectively. It was recorded that mean RAR at 1.5

m distance was 0.03% for *C. betulus* and 0.01% for *F. orientalis* (Fig. 8). Indeed, roots were detected for the 49.21% at the 1 m distance for *C. betulus* and 82.93% for *F. orientalis*. Only 20.80% and 10.76% of roots were distributed at 1.5 m distance for *C. betulus* and *F. orientalis*. It was noted that mean values of RAR at the 0-10 cm soil depth were 0.11 and 0.08% for *C. betulus* and *F. orientalis*, respectively (Fig. 8). In the case of 10-20 cm soil depth, it was estimated 0.06% for *C. betulus* and 0.02% for *F. orientalis* (Fig. 8). Approximately, in the case of *C. betulus*, 50% of roots distributed at the 0-10 cm soil depth and 69% for *F. orientalis*. Furthermore, at a depth of 10-20 cm, root distribution was reported 25.55% and 19.77% for *C. betulus* and *F. orientalis*, respectively. Overall, root distribution decreases with increasing soil depth and distance from the tree trunk. Moreover, root distribution was found higher on *C. betulus* than *F. orientalis*.

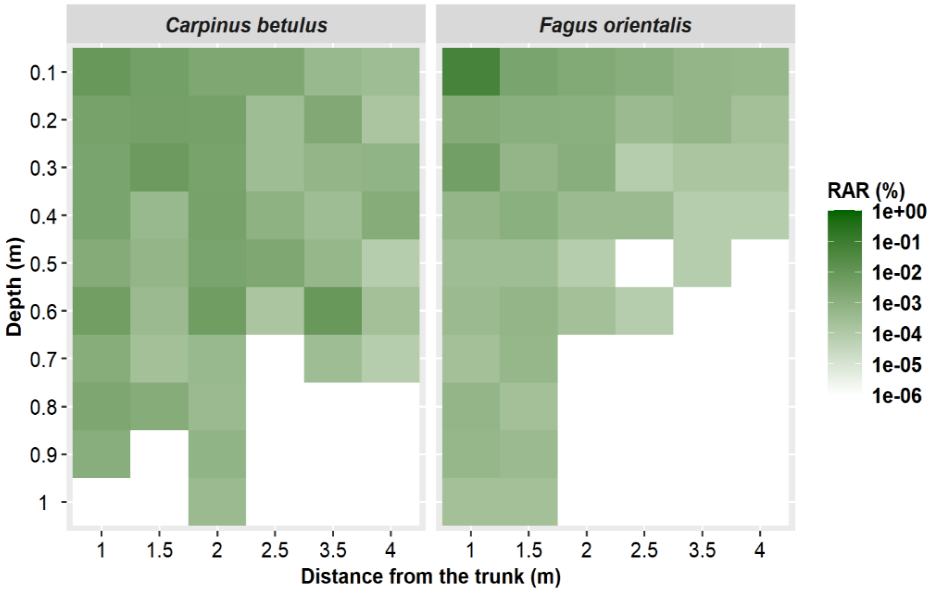

Fig. 8 Spatial distribution of Root Area Ratio (RAR in %) as a function of vertical and horizontal direction of *Carpinus betulus* and *Fagus orientalis*

3.2. Variability of the mechanical properties of roots

3.2.1. Variability of RBMw parameters

The main input parameters, including the relationship between root tensile force and root diameter, the regression coefficients for Young's modulus, root elongation, and the Weibull survival function are shown in Figures S2, S3, S4, S5, S6, S7, and Table S7. The results of the root tensile tests indicated strong relations between the mechanical and geometrical characteristics of the roots (root diameter) by power-law regression (Figs. S2-S7). Variability of Root Bundle Model Weibull (RBMw) parameters, including coefficients F_0, E_0, L_0 and exponents ξ, β, α, λ, ω were shown in Fig. 9. F_0 ranged between 12.41 and 124.18 N, E_0 ranged between 13.93 and 127.34 MPa, and L_0 ranged between 12.56 and 98.07 mm (Fig. 9). The minimum values of ξ, β, α, λ, ω were 0.94, -1.17, -0.48, 1.04, and 1.59, respectively. The maximum values of these exponents were 1.38, -0.64, -0.18, 1.39, and 4.29, respectively (Fig. 9).

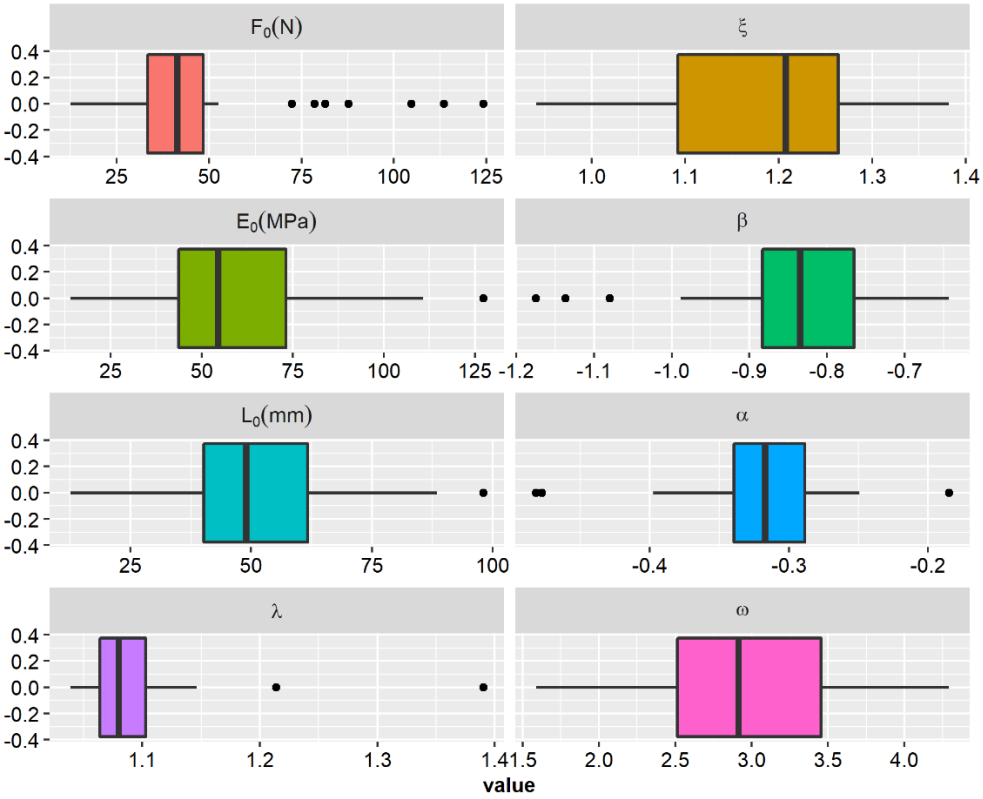

340

341 **Fig. 9** Variability of Root Bundle Model Weibull (RBMw) parameters: constant coefficients F_0, E_0, L_0 and exponents
342 ξ, β, α, λ, ω coefficients (unitless)

343 **3.2.2. Species-specific root reinforcement using RBMw model**

344 The mean values of root reinforcement for *C. betulus* and *F. orientalis* were of 16.08 kPa and 7.69 kPa, respectively.
345 Figure 10 showed that root reinforcement of *C. betulus* is higher at shallow depths than *F. orientalis*, whereas the
346 Kruskal-Wallis test showed a statistically significant difference in root reinforcement between the species ($H_1 = 168.22$,
347 $p < 2.2e\text{-}16$; Table S6). The minimum and maximum values of root reinforcement for *C. betulus* were calculated as
348 0.23 kPa and 216.95 kPa, respectively which is concentrated in shallower soil layers and nearer to the tree trunk. Root
349 reinforcement for *F. orientalis* varied from 0.07 to 145.39 kPa.

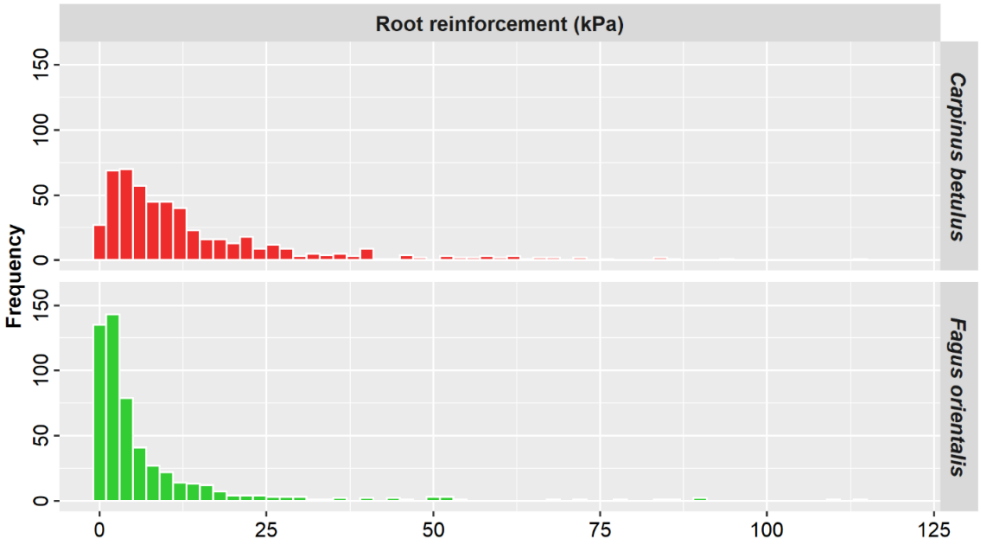

Fig. 10 Root reinforcement in function of species (*Carpinus betulus* and *Fagus orientalis*)

3.2.3. Impacts of environmental factors on RBMw-calculated root reinforcement

Applying RBMw, the root reinforcement of *C. betulus* was the highest in 400 m and 950 m compared with 1300 m. The mean values of c_r showed larger variation, including 23.89, 12.95, and 11.41 kPa at 400, 950, and 1300 m, respectively. Conversely, the mean value of c_r for *F. orientalis* reported 5.65, 9.58, and 7.85 kPa at the same altitudes, respectively. The results showed that c_r declined by decreasing DBH for both species (Fig. 11). Mean values of c_r reached 29.12, 14.29, and 4.82 kPa for large, medium and small trees of *C. betulus*, respectively; however, for the same DBH classes, the mean values of c_r for *F. orientalis* were of 15.52, 5.30, and 2.26 kPa, respectively. Furthermore, the c_r decreased with increasing distance from the tree trunk (Fig. 11). The highest mean value of c_r for *C. betulus* was of 38.55 kPa at 1 m distance from the tree, whereas it was of 26.99 kPa for *F. orientalis* at the same distance (Fig. 11). The lowest mean values of c_r were of 5.85 and 0.78 kPa, and they were found at distances of 4 m for *C. betulus* and *F. orientalis*, respectively (Fig. 11).

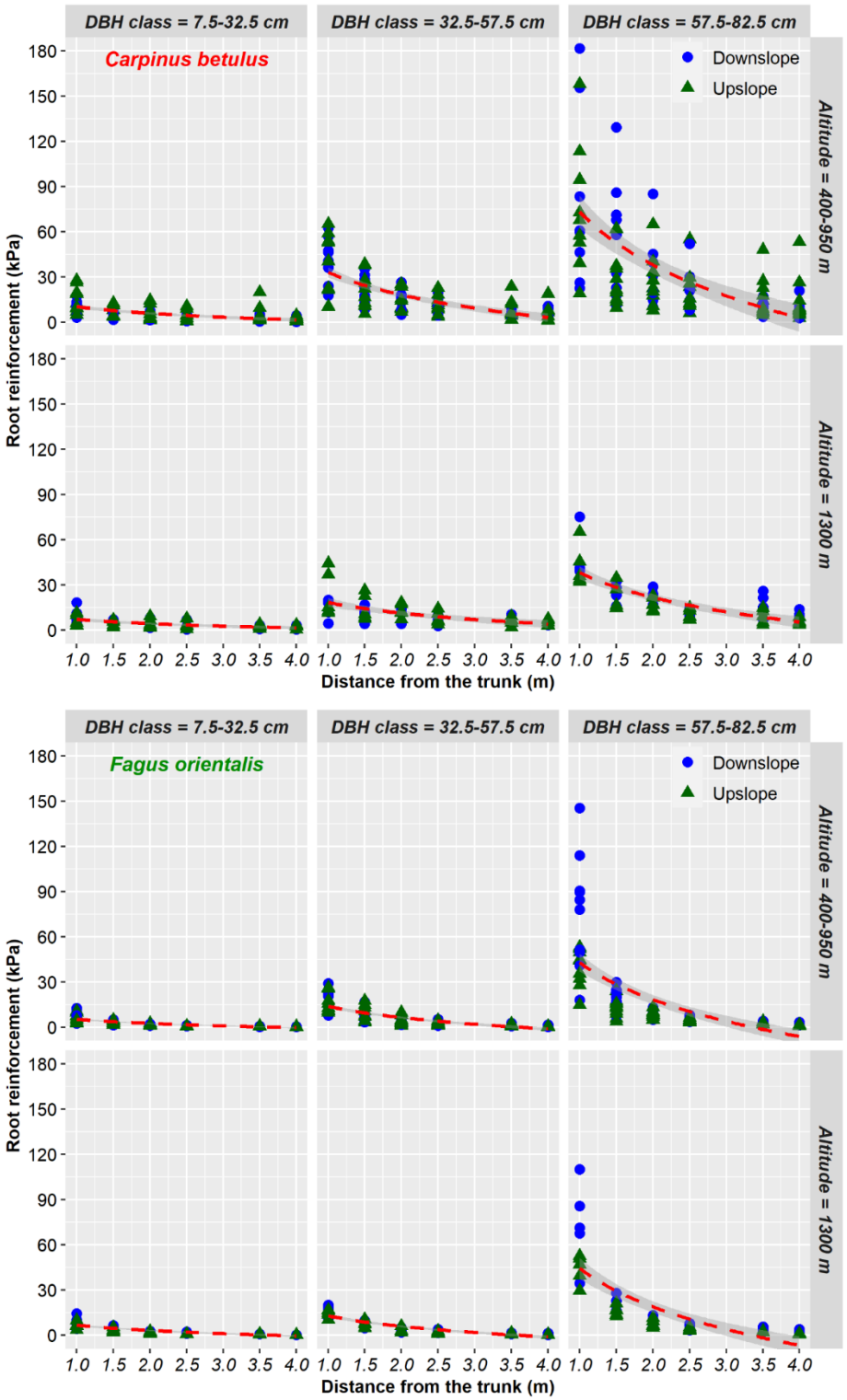

Fig. 11 Root reinforcement of *Carpinus betulus* and *Fagus orientalis* as a function of DBH class (small: 7.5-32.5 cm, medium: 32.5-57.5 cm, and large: 57.5-82.5 cm), altitudes (400, 950, and 1300 m a.s.l), and distance from tree (1, 1.5, 2, 2.5, 3.5, and 4 m)

3.3. Slope stability analysis

Including both basal and lateral reinforcement, the results of slope stability analysis (Eq. 7) suggested that the most stabilizing species is *C. betulus* in a mature growth (DBH= 57.5-82.5 cm) at the distance of 4 m. In fact, at 400, 950, and 1300 m a.s.l trees of *C. betulus* maintained an instability probability near 18.3%, 23.6%, and 29.9% for very steep conditions, respectively (Fig. 12). Instability probability for small trees at same altitudes varied from 37.8% to 40.6%. These values for medium trees of *C. betulus* were reported between 26.8% and 31.9% (Fig. 12). In contrast, the instability probabilities of the *F. orientalis* was higher, reaching up to approximately 44.0% for all DBH classes at 400, 950, and 1300 m a.s.l (Fig. 12). The instability probabilitiy was less than 10% until 40° for *F. orientali*s at a distance of 4 m (Fig. 12).

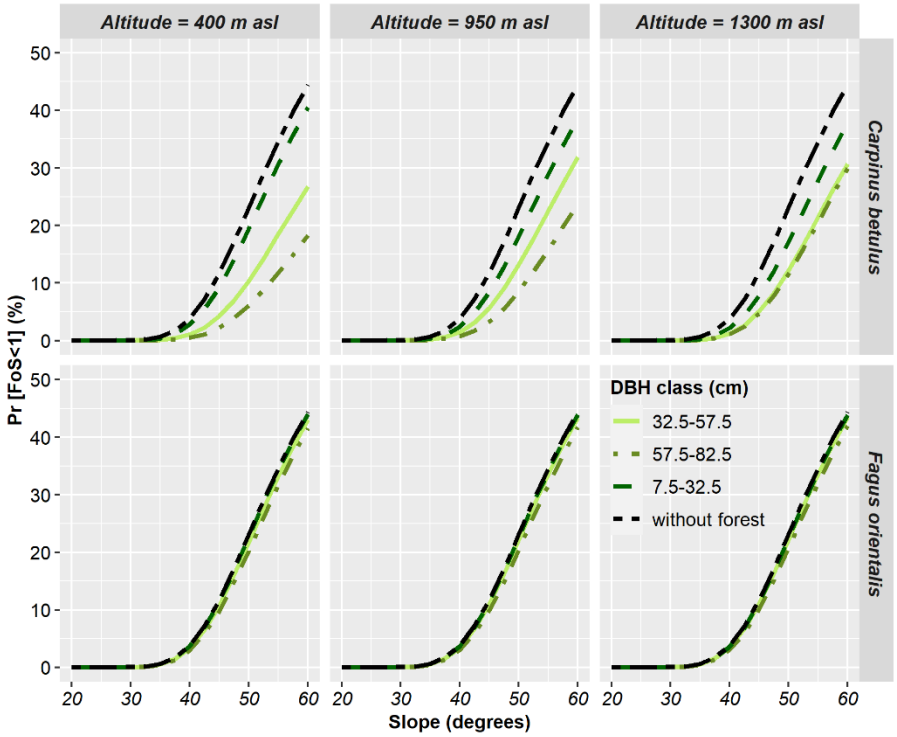

Fig. 12 Factor of safety (*FoS*), probability of failure (Pr(FoS < 1)), in function of species (*Carpinus betulus* and *Fagus orientalis*), altitude (400, 950, and 1300 m a.s.l.), and DBH classes (small: 7.5-32.5 cm, medium: 32.5-57.5 cm, and large: 57.5-82.5 cm) considering the upslope position and the far distance from the trunk (i.e. 4 m). In all the cases, the contribution to slope stability by the vegetation is evaluated as the sum of both basal and lateral root reinforcement values

4. Discussion

4.1. Root distribution

The scientific literature often used RAR to quantify, first, root distribution into the soil and, second, root reinforcement. The root density, measured as a total number of roots per unit area and RAR, was significantly different between the two investigated species. Root density of *C. betulus* was higher than that of *F. orientalis*. This observation is consistent with previous literature, showed that root density is different amongst tree species growing under the same environmental conditions, suggesting a genetic control on rooting densities (Bischetti et al. 2007; Phillips et al. 2014; Vergani et al. 2017a; Moresi et al. 2019; Gholami-Derami et al. 2021). For example, Bischetti et al. (2007) found differences among European alpine species, including *Alnus viridis*, *Fagus sylvatica*, *Salix purpurea*, *Salix caprea*, *Corylus avellana*, *Fraxinus excelsior*, *Picea abies*, and *Larix decidua* in which root density varies significantly for the same species within the same locality. Gholami-Derami et al. (2021) compared the RAR of *C. betulus* with that of *Alnus subcordata* and among two non-native tree species (*Pinus sylvestris* and *Robinia pseudoacacia*) with similar habitat conditions in Northern Iran. They found that the RAR value in exotic species is higher than in native species. A study in New Zealand reported that willow roots were more numerous than poplar (Phillips et al. 2014). Stokes et al. (2008) found that this variability was related to the interactions of genetic and environmental factors. Hence it is likely that these genetic effects are compounded by heterogeneity in environmental factors (Burylo et al. 2011), such as soil bulk density (Goodman and Ennos 1999), and soil moisture and fertility (Taub and Goldberg 1996; Hodge 2004).

Older trees with larger DBH, have a greater number of roots than younger trees with smaller diameters (Bischetti et al. 2009; Schwarz et al. 2010; Mehtab et al. 2021). Abdi et al. (2010b) showed a significant effect of DBH on total RAR in three hardwood species in Hyrcanian forests (*F. orientalis*, *C. betulus*, and *Parrotia persica*). In accordance, John et al. (2001), comparing three stands of 6, 15, and 23 years old, showed that root distribution increases by tree age. Additionally, it was reported that in the older stands, fine roots (0-2 mm) declined, which they interpreted as a conversion to coarse roots (>10 mm) to provide structural support (John et al. 2001). McQueen (1968) reported that fine roots peak at the early ages of the stands and are relatively maintained constant after that. Our findings are consistent with these observations that larger trees maintain their anchorage, with increasing root numbers and RAR values. In fact, nutrient availability increases lateral root extension as well as causes changes in lateral roots anatomy by supplying nutrients (Goss et al. 1993). Also, Ford and Deans (1977) reported a higher concentration of fine roots because of increased nutrient availability. Past research suggested that greater root biomass was allocated to areas of high soil moisture content (Sivandran and Bras 2013; Hales and Miniat 2017). Furthermore, in this study, soil moisture content can be considered as a plausible factor in the distribution of roots.

So, greater root mass could be attributed to the higher nutrient content and better aeration of the surface soil (Ford and Deans 1977). Overall, root growth can be affected by a variety of environmental factors such as soil texture, soil structure, aeration, moisture, temperature, and competition with other plants (Kramer and Boyer 1995).

The position of the roots with respect to the orientation of the tree on the slope influences root distribution with the increased role of root upslope of the stem in assisting soil anchorage (Vergani et al. 2017a), as observed in this study for *F. orientalis* species. RAR distribution of *F. orientalis* in downslope is greater than upslope; however, in the case of *C. betulus*, the RAR values of both slopes were similar. The difference in the mechanical function of the root system in downslope and upslope orientations depends on the specific type of root system architecture (i.e., asymmetry of the cross-sectional area; Chiatante et al. 2003). Higher mechanical stresses being applied to roots may explain the large

cross-sectional areas (Di Iorio et al. 2005), therefore, the higher RAR value of *F. orientalis* in downslope is a kind of adaptability in response to the environment. In the case of *C. betulus*, RAR values of downslope and upslope were not significantly different, probably implying that trees are thickening the roots instead of increasing the number in the reaction of the mechanical stresses (Abdi et al. 2010a).

Our results highlighted that RAR values fluctuate among different altitudes, and RAR in the 1300 m is higher than 950 and 400 m. One possible reason is the variation among the meteorological parameter and altitude above sea level. These altitudes range from low altitude (i.e., 400 m a.s.l.) with the highest mean temperature and lowest annual precipitation to mid- altitude (i.e., 950 m a.s.l.) to the highest altitude (i.e., 1300 m a.s.l.) having the lowest mean air temperature and greatest annual precipitation with the most proportion of snowfall (Azaryan et al. 2015; Deljouei et al. 2020). Bischetti et al. (2009) showed that for *F. sylvatica*, RAR distributions were statistically more in a site with the highest altitude than the lowest altitude (altitude ranges from 1100 to 1454 m a.s.l.). Mao et al. (2012) found similar results for *P. abies*, *Abies alba*, and *F. sylvatica* growing at 1400 m a.s.l. and 1700 m a.s.l. The use of altitude gradients is considered an excellent way to examine vegetation responses to environmental change (Sundqvist et al. 2013; Weemstra et al. 2021). Higher altitudes in temperate regions typically have longer growing seasons and more seasonality, and their vegetation is adapted to the extreme variations in climate they can experience (Körner 1999; Sundqvist et al. 2013). In most cases, high-altitude soils are more heterogeneous in terms of soil nutrient availability (Holtmeier and Broll, 2005) and less fertile (Sveinbjörnsson et al. 1995), since the cooler temperatures slow down microbial activity (Loomis et al. 2006; Mayor et al. 2017), leaf and root litter decomposition rates (Moore 1986; Loomis et al. 2006; See et al. 2019), and mineralization rates (Sveinbjörnsson et al. 1995). This means that changes in climate and soil properties along an altitude gradient can profoundly influence intraspecific root trait variation (Weemstra et al. 2021).

Another significant factor is the distance from the trunk. In fact, root distribution decreases with increasing distance from tree trunk and soil depth for both species. Seventy percent of *C. betulus* roots and 94% *F. orientalis* roots were distributed at a 1.5 m distance from the tree trunk. Furthermore, the maximum RAR values (50% of *C. betulus* roots and 69% of *F. orientalis* roots) were situated in the surface soil, i.e. 1-10 cm of soil depth and approximately were smaller in deeper soil. Species or genetics, climate characteristics determined root distribution throughout the soil profiles, and soil type (Bischetti et al. 2005); for instance, changes in nutrient content, water availability and aeration will affect root distribution, whereas the most available nutrients are detected in the topsoil and cause a reduction in vertical root distribution (Bischetti et al. 2005; Abdi et al. 2010a; Mao et al. 2012; Bordoni et al. 2019; Moresi et al. 2019). It was pointed out that root development might depend mainly on the quantity of organic matter in the soil (Bordoni et al. 2019). In addition, deeper layers due to compacted soil layers and bedrock caused the roots to grow horizontally (Coppin and Richards 1990; Zydroń et al. 2019). The decreasing pattern of RAR values in this study is similar to the values reported by other researchers for various species and in other locations such as the Mediterranean (Moresi et al. 2019), subtropical (Genet et al. 2008), temperate (Bischetti et al. 2005; Abdi et al. 2010a; Abdi and Deljouei 2019), arid (Abdi et al. 2019) climate zones.

4.2. Root reinforcement

Root reinforcement is fundamentally determined by combining root distribution and mechanical properties (Schwarz et al. 2013). Mechanical properties of roots are well-known by root maximum tensile force and stiffness. Several researchers indicated that different parameters affect root resistance, including species (Abdi and Deljouei 2019), root size and age (Loades et al. 2013; Gilardelli et al. 2017; Boldrin et al. 2017), tree age (Genet et al. 2008), root length (Zhang et al. 2012), DBH (Deljouei et al. 2020), cellulose and lignin content (Hales et al. 2009; Abdi et al. 2014), root moisture content (Hales & Miniat et al. 2017; Moresi et al. 2019), root dehydration (Ekeoma et al. 2021), season (Makarova et al. 1998; Abdi and Deljouei 2019), living or decaying roots (Vergani et al. 2014), altitude (Genet et al. 2011), slope position (Stokes 2002; Abdi et al. 2010a), soil moisture content (Tsige et al. 2020), and elastic modulus as a root reinforcement input parameter (Cislaghi 2021).

The mechanical properties of roots may vary according to environmental conditions and tree location, where roots resistance will be varied by different altitudes or topographic positions (Genet et al. 2011; Hales et al. 2009). Altitude may cause differences in root cellulose content that alter root resistance. Systematic changes in environmental conditions (particularly altitude) might then result in systematic changes to root reinforcement that can be incorporated into deriving better root models. Root reinforcement of *C. betulus* at 400 m a.s.l. is higher than 1300 m a.s.l, i.e. root reinforcement decreased significantly with increasing altitude, which means it required more force for root failure. These findings are similar to other studies performed on root reinforcement of different altitudes (Genet et al. 2011; Vergani et al. 2012). It was investigated that the differences in site interactions for various species result from several conditions of growing sites and environment (Vergani et al. 2012). It is clarified that soil's chemical and physical properties are a consequence of changes in root resistance and root reinforcement with increasing altitude (Genet et al. 2011).

The quantity of root reinforcement assessed by the contribution of different species might indicate the impact of roots in reducing shallow landslides and slope instabilities. Root numbers of *C. betulus* were more numerous than *F. orientalis*, so root reinforcement of *C. betulus* is higher than *F. orientalis*. Also, root resistance has differed between altitudes, and roots of *C. betulus* have shown higher resistance in terms of force than *F. orientalis* (see Deljouei et al. 2020).

Root reinforcement of large trees is the highest among all the tree DBH classes, concurs with Cohen and Schwarz (2017). The roots of the oldest trees were the most resistant in tension compared to the middle age and young trees (Genet et al. 2006). It could be defined by the differences in the root structure of trees in the early growth stage and older trees, as large DBH trees may possess a higher amount of cellulose (Genet et al. 2006). As a result, investigating cellulose content in roots of large, medium, and small trees would be interesting in future research.

Root reinforcement decreases with increasing distance from tree trunks and varies considerably, even at the same distance from trees, and similar results were found in past research (Moos et al. 2016). Therefore, we highlighted that considering uniform cohesion value for vegetation in landslide models may not be appropriate to represent the effect of trees on slope stability.

4.3. The implications on slope stability and possible countermeasures of forest management

Our work shows that there are systematic differences in root reinforcement based on DBH, distance from the tree trunk, and altitude, with tree species and slope position adding random variability. Hence, when defining the magnitude of cohesion term for vegetation in physically-based landslide models (e.g., CHASM model (Wilkinson et al. 2002), TRIGRS model (Baum et al. 2008), SOSlope model (Cohen and Schwarz 2017), PRIMULA model (Cislaghi et al. 2018), and SLIP model (Montrasio and Valentino 2008)) systematic accounting of this variability has yet to be formally attempted. Our results show that root reinforcement approximately halved across 1000 m of altitude, however this effect may not be linear. DBH had a greater effect, with close to an order of magnitude reduction in root reinforcement between large and small trees. Similarly, there is close to an order of magnitude reduction in root reinforcement between 1 and 4 m from the trunk. In contrast, there was no systematically observed differences in root reinforcement between species or in upslope and downslope positions. The distance from trunk showed a significant effect on the estimation of root reinforcement. For practical application, we conducted the analysis on the hillslope stability considering the most conservative quantification of root reinforcement, i.e., at 4 m of distance. This choice can simulate a forest disturbance as a gap-opening due to gap-oriented forestry operation, uprooting trees by windstorm, snags, or dead trees hit by bark beetle attack. This work outlines how a simple model of root reinforcement could be built that better incorporates environmental controls and crown or trunk properties. Given the large uncertainties present in the root reinforcement term (Hales 2018), our work shows that for raster-based estimates of slope stability, incorporation of an altitude term will better constrain the cohesion values. However, higher resolution slope stability modelling may benefit from more sophisticated root cohesion applications based on the relationship between DBH and root crown shape and depth.

By comparing the performance of various species in terms of additional root reinforcement, the species most likely to increase slope stability were identified. Also, our result can be used for nature-based solutions targeting root reinforcement, like the effect of different forest stand structures on slope stability (Moos et al. 2016; Dazio et al. 2018), and forest management scenarios (Kumar et al. 2021). Over a long period, *C. betulus* is preferable to *F. orientalis* when promoting one species over another to increase (or maintain) slope stability. Forest managers should consider this outcome when developing strategies for large forests in mountainous areas. Certainly, factors including inter-and intraspecific competition affect the performance of species concerning slope stability (Chiaradia et al. 2016). As shown in this paper, this performance can be considered by using a large, widely distributed dataset and evaluating the probabilistic function used to describe the values in the field survey. By clarifying the higher prevention power's behaviour from large DBH *C. betulus* trees, it is possible to propose forest management that keep this tree species with a large diameter in landslide-prone areas. Using both basal and lateral reinforcement, the results suggest that the most stabilizing species is *C. betulus*. Importantly, our findings imply tree diameter and species may be appropriate for assessing FoS by common tree species in Hyrcanian temperate forests. Future studies can be conducted on the available landslide inventory data with back analysis.

4.4. Research limitations

As a first limitation, we could not conduct our study on other parts of Hyrcanian temperate forests due to financial limitations; However, to overcome this limitation, 540 profile trenches were dug for each species (compared to 10

(Abdi et al. 2010a, b), 24 (Vergani et al. 2017 b; Abdi and Deljouei 2019), 33 (Vergani et al. 2014) profile trenches for each species in previous studies in the temperate region). Also, ground-truthing of many parameters (e.g., dimensions of slope failures) is advisable for slope stability modelling. Many parameters were calculated based on previous literature rather than measured (second limitation). Last but not least, it is worth commenting on the computation time. Due to a lack of instrumentation or measurement difficulties, there are sometimes difficulties accessing datasets (e.g., geotechnical, geomorphological, and forest structural inputs) for complex slope stabilization models.

5. Conclusions

This study conducted a total of 1080 profile trenches for widely species in temperate forests of Iran and European countries (i.e., *C. betulus* and *F. orientalis*) at various altitudes (i.e., 400, 940, and 1350 m a.s.l.). Root distribution and mechanical properties of trees with 7.5-32.5, 32.5-57.5, and 57.5-82.5 cm DBH were used as input parameters of RBMw. This study highlighted quantitative information about the impact of roots mechanical properties and distribution in DBH classes, slope position, altitude, and vertical and horizontal distance from tree trunk of *C. betulus* and *F. orientalis* on root reinforcement and slope stability is the practical conjunction for forest management. Our results reported that altitude, DBH classes, and slope position significantly affect root reinforcement in Hyrcanian temperate forests. Slope stabilization is decreased in further distances (more than 1 m) from the tree trunk; furthermore, it is entirely different for both species in which *C. betulus* shows better root reinforcement than *F. orientalis*. Furthermore, the most stabilizing species is mature *C. betulus* at all altitudes, which maintained an instability probability near 29% for very steep conditions. Overall, we could highlight that vegetation's impact on soil slope stability depends on various parameters, and considering the constant value of soil reinforcement via tree roots in soil stabilization modelling is incorrect. As far as slope stabilization is concerned, there are no specific species suitable for all ecological conditions since its suitability depends not only on its root reinforcement characteristics but also on the species ability to grow and support healthy forest cover. Protecting slopes from long-term instability is dependent on the forest's ability to withstand disturbances and its ability to recover after disturbances.

Appendix A

This appendix summarises the equations included in PRIMULA. The driving and resistance forces, reported in Eq. 7, are described as follows.

- Soil weight and tree surcharge force acting downslope, F_{dc}:

$$F_{dc} = \{[\gamma_s(1-m) + (\gamma_s + \gamma_w)m]D + q_0\} \cos\theta \sin\theta \, wl \quad \text{(A.1)}$$

where γ_s is the unit weight of soil (Nm^{-3}), γ_w is the unit weight of water (Nm^{-3}), m is the saturation ratio (unitless), i.e., the ratio between the thickness of the saturated part of the sliding soil D_w (in m) and the soil depth of sliding surface D (in m), θ is the surface slope (rad), q_0 is the tree surcharge (Nm^{-2}), w is the potential landslide width, and l is the potential landslide length (m).

- Rooted-soil shear resistance on the two parallel cross-slope sides of the sliding block, F_{rl}:

$$F_{rl} = \frac{1}{2}K_0[(\gamma_s - \gamma_w m^2)z^2 + q_0]\cos\theta\, l \tan\varphi' + (C_s' + C_{rl}')lz \quad (A.2)$$

where K_0 is the at-rest earth coefficient, q_0 is the forested soil surcharge at the lateral boundary, φ' is the internal friction angle of soil (rad), C_s' is the effective soil cohesion (Nm^{-2}), C_{rl}' is the lateral root reinforcement (Nm^{-2}), and z is failure depth.

$$K_0 = 1 - \sin\varphi' \quad (A.3)$$

- Root tensile resistance on the upslope side of the sliding block, F_{ru}:

$$F_{ru} = C_{rl}' wz\cos\theta \quad (A.4)$$

- Slope-parallel component of passive earth force, F_{rd}:

$$F_{rd} = \frac{1}{2}K_p[(\gamma_s - \gamma_w m^2)z^2 + q_0]w\cos(\delta - \theta) \quad (A.5)$$

where K_p is the passive earth coefficient (unitless), and δ is the friction angle along the failure surface (rad). In this case, we assumed $\delta = \theta$.

- Slope-parallel component of active earth force, F_{du}:

$$F_{du} = \frac{1}{2}K_a\ [(\gamma_s - \gamma_w m^2)\ z^2 + q_0\ ]\ w\ \ cos(\delta - \theta) \quad (A.6)$$

where K_a is the active earth coefficient (unitless). K_p and K_a are evaluated according to the Rankine theory for cohesive soils proposed by Mazindrani and Ganjali (1997) and verified by Cislaghi et al. (2019).

- Frictional resistance and rooted-soil cohesion acting on the sliding block base, F_{rb}:

$$F_{rb} = \left(C_s' + C_{rb}'\right)wl + F_{nt}\tan\varphi' \quad (A.7)$$

where C'_{rb} is the basal root reinforcement (Nm^{-2}) and F_{nt} is the total effective normal force acting on the failure surface.

$$F_{nt} = \{[\gamma_s(1-m) + \gamma_{sat}m]z + q_0 - \gamma_w mz\}wl\cos^2\theta + \frac{1}{2}\left(K_a - K_p\right)[(\gamma_s - \gamma_w m^2)z^2 + q_0]w\cos(\delta - \theta) \quad (A.8)$$

where γ_{sat} is the unit weight of soil (Nm^{-3}) that is estimated by considering that all the voids are 40% of the total volume and are filled by water (Hammond et al. 1992; Chiaradia et al. 2016).

References

Abbaszadeh Shahri A, Maghsoudi Moud F (2021) Landslide susceptibility mapping using hybridized block modular intelligence model. Bull Eng Geol Environ 80:267–284. https://doi.org/10.1007/s10064-020-01922-8

Abdi E, Azhdari F, Abdulkhani A, Mariv HS (2014) Tensile strength and cellulose content of Persian ironwood (*Parrotia persica*) roots as bioengineering material. J For Sci 60:425–430. https://doi.org/10.17221/44/2014-JFS

Abdi E, Deljouei A (2019) Seasonal and spatial variability of root reinforcement in three pioneer species of the Hyrcanian forest. Austrian J For Sci 136:175–198

583 Abdi E, Majnounian B, Genet M, Rahimi H (2010a) Quantifying the effects of root reinforcement of Persian Ironwood
584 (*Parrotia persica*) on slope stability; a case study: Hillslope of Hyrcanian forests, northern Iran. Ecol Eng 36:1409–
585 1416. https://doi.org/10.1016/j.ecoleng.2010.06.020

586 Abdi E, Majnounian B, Rahimi H, Zobeiri M, Mashayekhi Z, Yosefzadeh H (2010b) A comparison of root distribution
587 of three hardwood species grown on a hillside in the Caspian forest, Iran. J For Res 15: 99–107.
588 https://doi.org/10.1007/s10310-009-0164-2

589 Abdi E, Saleh HR, Majnounian B, Deljouei A (2019) Soil fixation and erosion control by *Haloxylon persicum* roots in
590 arid lands, Iran. J Arid Land 11:86–96. https://doi.org/10.1007/s40333-018-0021-2

591 Arnone ED, Caracciolo D, Noto LV, Preti F, Bras RL (2016) Modeling the hydrological and mechanical effect of roots
592 on shallow landslides. Water Resources Research 52:8590–8612. https://doi.org/10.1002/2015WR018227

593 Azaryan M, Marvie-Mohadjer MR, Etemaad V, Shirvany A, Sadeghi SMM (2015) Morphological characteristics of
594 old trees in Hyrcanian forest (Case study: Pattom and Namkhaneh districts, Kheyrud). J For Wood Prod 68:47–59.
595 https://doi.org/10.22059/JFWP.2015.53977

596 Baum RL, Savage WZ, Godt JW (2008) TRIGRS: a Fortran program for transient rainfall infiltration and grid-based
597 regional slope-stability analysis. US Geological Survey open-file report 424:38.

598 Bischetti GB, Chiaradia EA, Simonato T, Speziali B, Vitali B, Vullo P, Zocco A (2005) Root strength and root area of
599 forest species in Lombardy. Plant Soil 278:11–22. https://doi.org/10.1007/978-1-4020-5593-5_4

600 Bischetti GB, Chiaradia EA, Epis T, Moriotti E (2009) Root cohesion of forest species in the Italian Alps. Plant Soil
601 324:71–89. https://doi.org/10.1007/s11104-009-9941-0

602 Bischetti GB, Chiaradia EA, Simonato T, Speziali B, Vitali B, Vullo P, Zocco A (2007) Root strength and root area
603 ratio of forest species in Lombardy (Northern Italy). In: Stokes A, Spanos I, Norris JE, Cammeraat E (eds) Eco-and
604 Ground Bio-Engineering: The Use of Vegetation to Improve Slope Stability. Developments in Plant and Soil Sciences,
605 vol 103. Springer, Dordrecht. https://doi.org/10.1007/978-1-4020-5593-5_4

606 Boldrin D, Leung AK, Bengough AG (2017) Correlating hydrologic reinforcement of vegetated soil with plant traits
607 during establishment of woody perennials. Plant Soil 416: 437–451. https://doi.org/10.1007/s11104-017-3211-3

608 Bordoni M, Vercesi A, Maerker M, Ganimede C, Reguzzi MC, Capelli E, Wei X, Mazzoni E, Simoni S, Gagnarli E,
609 Meisina C (2019) Effects of vineyard soil management on the characteristics of soils and roots in the lower Oltrepò
610 Apennines (Lombardy, Italy). Sci Total Environ 693:133390. https://doi.org/10.1016/j.scitotenv.2019.07.196

611 Burylo M, Hudek C, Rey F (2011) Soil reinforcement by the roots of six dominant species on eroded mountainous
612 marly slopes (Southern Alps, France). Catena 84: 70–78. https://doi.org/10.1016/j.catena.2010.09.007

613 Böhm W, (1979) Methods of studying root systems, Ecological Studies. Springer, Berlin, Germany

614 Casadei M, Dietrich WE, Miller N (2003) Controls on shallow landslide size. In: Proceedings of the 3rd International
615 Conference on Debris-Flow Hazards Mitigation: Mechanics, Prediction, and Assessment. Davos, Swizerland.

616 Chiaradia EA, Vergani C, Bischetti GB (2016) Evaluation of the effects of three European forest types on slope
617 stability by field and probabilistic analyses and their implications for forest management. For Ecol Manag 370:114–
618 129. https://doi.org/10.1016/j.foreco.2016.03.050

619 Chiatante D, Sarnataro M, Fusco S, Di Iorio A, Scippa GS (2003) Modification of root morphological parameters and
620 root architecture in seedlings of *Fraxinus ornus* L. and *Spartium junceum* L. growing on slopes. Plant Biosyst 137:47–
621 55. https://doi.org/10.1080/11263500312331351321

622 Cislaghi A (2021) Exploring the variability in elastic properties of roots in Alpine tree species. J For Sci 67: 338–356.
623 http://dx.doi.org/10.17221/4/2021-JFS

624 Cislaghi A, Bordoni, M, Meisina, C, Bischetti, GB (2017) Soil reinforcement provided by the root system of
625 grapevines: Quantification and spatial variability. Ecological Engineering 109: 169–185.

626 Cislaghi, A, Cohen, D, Gasser, E, Bischetti, GB, Schwarz, M (2019) Field measurements of passive earth forces in
627 steep, shallow, landslide-prone areas. Journal of Geophysical Research: Earth Surface 124(3):838–866.

628 Cislaghi A, Rigon E, Lenzi MA, Bischetti GB (2018) A probabilistic multidimensional approach to quantify large
629 wood recruitment from hillslopes in mountainous-forested catchments. Geomorphology 306:108–127.
630 https://doi.org/10.1016/j.geomorph.2018.01.009

631 Cislaghi A, Alterio E, Fogliata P, Rizzi A, Lingua E, Vacchiano G, Bischetti GB, Sitzia T (2021) Effects of tree spacing
632 and thinning on root reinforcement in mountain forests of the European Southern Alps. For Ecol Manag 482:118873.
633 https://doi.org/10.1016/j.foreco.2020.118873

634 Cohen D, Schwarz M (2017) Tree-root control of shallow landslides. Earth Surf Dynamics 5(3):451-477.
635 https://doi.org/10.5194/esurf-5-451-2017

636 Coppin NJ, Richards IG (1990) Use of vegetation in civil engineering. Butterworth, London

637 Dazio EPR, Conedera M, Schwarz M (2018) Impact of different chestnut coppice managements on root reinforcement
638 and shallow landslide susceptibility. Forest Ecology and Management 417:63–76.
639 https://doi.org/10.1016/j.foreco.2018.02.031

640 Deljouei A, Abdi E, Schwarz M, Majnounian B, Sohrabi H, Dumroese RK (2020) Mechanical characteristics of the
641 fine roots of two broadleaved tree species from the Temperate Caspian Hyrcanian Ecoregion. Forests 11:345.
642 https://doi.org/10.3390/f11030345

643 Di Iorio A, Lasserre B, Scippa GS, Chiatante D (2005) Root system architecture of *Quercus pubescens* trees growing
644 on different sloping conditions. Ann Bot 95:351–361. https://doi.org/10.1093/aob/mci033

Ekanayake JC, Phillips CJ (1999) A method for stability analysis of vegetated hillslopes: an energy approach. Can Geotech J 36:1172–1184. https://doi.org/10.1139/t99-060

Ekeoma EC, Boldrin D, Loades KW, Bengough AG (2021) Drying of fibrous roots strengthens the negative power relation between biomechanical properties and diameter. Plant Soil 1–14. https://doi.org/10.1007/s11104-021-05150-1

Endo T, Tsuruta T (1969) Effects of tree root upon the shearing strengths of soils. Annual Report of the Hokkaido Branch, Tokyo Forest Experiment Station 18:168–179.

Farahnak M, Mitsuyasu K, Jeong S, Otsuki K, Chiwa M, Sadeghi SMM, Kume A (2019) Soil hydraulic conductivity differences between upslope and downslope of two coniferous trees on a hillslope. J Forest Res 24(3):143-152. https://doi.org/10.1080/13416979.2019.1590967

Fathizadeh O., Sadeghi SMM, Holder CD, Su L. (2020) Leaf phenology drives spatio-temporal patterns of throughfall under a single *Quercus castaneifolia* CA Mey. Forests 11(6):688. https://doi.org/10.3390/f11060688

Ford ED, Deans JD (1977) Growth of a sitka spruce plantation: spatial distribution and seasonal fluctuations of lengths, weights and carbohydrate concentration of fine roots. Plant Soil 47:463–485. https://doi.org/10.1007/BF00011504

Gehring E, Conedera M, Maringer J, Giadrossich F, Guastini E, Schwarz M (2019) Shallow landslide disposition in burnt European beech (Fagus sylvatica L.) forests. Sci Rep 9:8638. https://doi.org/10.1038/s41598-019-45073-7

Genet M, Kokutse N, Stokes A, Fourcaud T, Cai X, Ji J, Mickovski S (2008) Root reinforcement in plantations of *Cryptomeria japonica* D. Don: effect of tree age and stand structure on slope stability. Forest Ecol Manag 256:1517–1526. https://doi.org/10.1016/j.foreco.2008.05.050

Genet M, Stokes A, Fourcaud T, Norris JE (2010) The influence of plant diversity on slope stability in a moist evergreen deciduous forest. Ecological Engineering 36:265–275. https://doi.org/10.1016/j.ecoleng.2009.05.018

Genet M, Li M, Luo T, Fourcaud T, Clément-Vidal A, Stokes A (2011) Linking carbon supply to root cell-wall chemistry and mechanics at high altitudes in *Abies georgei*. Ann Bot 107: 311–320. https://doi.org/10.1093/aob/mcq237

Genet M, Stokes A, Fourcaud T, Hu X, Lu Y (2006) Soil fixation by tree roots: changes in root reinforcement parameters with age in *Cryptomeria japonica* D. Don. plantations. In Interpraevent 25–27

Gholami-Derami A, Akbari H, Nasiri M, Foshat M (2021) Comparison of bioengineering characteristics of native and non-native tree species. J Wood For Sci Technol 27:67–80. https://doi.org/10.22069/JWFST.2021.18253.1884

Giadrossich F, Cohen D, Schwarz M, Ganga A, Marrosu R, Pirastru M, Capra GF (2019) Large roots dominate the contribution of trees to slope stability. Earth Surf Process Landf 44:1602–1609. https://doi.org/10.1002/esp.4597

675 Giadrossich F, Schwarz M, Marden M, Marrosu R, Phillips C (2020) Minimum representative root distribution
676 sampling for calculating slope stability in *Pinus radiata* D. Don plantations in New Zealand. N Z J For Sci 50.
677 https://doi.org/10.33494/nzjfs502020x68x

678 Gilardelli F, Vergani C, Rodolfo G, Bonis A, Chanteloup P, Citterio S, Chiaradia EA (2017) Root characteristics of
679 herbaceous species for topsoil stabilization in restoration projects. Land Degrad Dev 28:2074–2085.
680 https://doi.org/10.1002/ldr.2731

681 Goodman AM, Ennos AR (1999) The effects of soil bulk density on the morphology and anchorage mechanics of the
682 root systems of sunflower and maize. Ann Bot 83:293–302. https://doi.org/10.1006/anbo.1998.0822

683 Goss MJ, Miller MH Bailey LD, Grant CA (1993) Root growth and distribution in relation to nutrient availability and
684 uptake. Eur J Agron 2:57–67. https://doi.org/10.1016/S1161-0301(14)80135-4

685 Gray DH, Sotir RB (1996) Biotechnical and soil bioengineering slope stabilization: a practical guide for erosion
686 control. John Wiley & Sons, New York, USA.

687 Haghshenas M, Mohadjer MRM, Attarod P, Pourtahmasi K, Feldhaus J, Sadeghi SMM (2016) Climate effect on tree-
688 ring widths of *Fagus orientalis* in the Caspian forests, northern Iran. For Sci Technol 12(4):176-182.
689 https://doi.org/10.1080/21580103.2016.1144542

690 Hales TC (2018) Modelling biome-scale root reinforcement and slope stability. Earth Surface Processes and
691 Landforms, 43(10):2157–2166. https://doi.org/10.1002/esp.4381

692 Hales TC, Miniat CF (2017) Soil moisture causes dynamic adjustments to root reinforcement that reduce slope
693 stability. Earth Surf Process Landforms 42(5):803–813. https://doi.org/10.1002/esp.4039

694 Hales TC, Ford CR, Hwang T, Vose JM, Band LE (2009) Topographic and ecologic controls on root reinforcement. J
695 Geophys Res 114. https://doi.org/10.1029/2008JF001168

696 Hammond C, Hall D, Miller S, Swetik P (1992) Level I Stability Analysis (LISA) Documentation for Version 2.0. US
697 Department of Agriculture, Forest Service, Intermountain Research Station

698 Hayati E (2017). Monitoring of forest slope hydrological changes for applying in hydrological and slope stability
699 models. PhD thesis, University of Tehran, Karaj, Iran.

700 Heshmatol Vaezin SM, Moftakhar Juybari M, Sadeghi SMM, Banaś J, Marcu MV (2022) The seasonal fluctuation of
701 timber prices in Hyrcanian temperate forests, northern Iran. Forests 13:761. https://doi.org/10.3390/f13050761

702 Hodge A (2004) The plastic plant: root responses to heterogeneous supplies of nutrients. New phytol 162: 9–24.
703 https://doi.org/10.1111/j.1469-8137.2004.01015.x

Holtmeier FK, Broll G (2005) Sensitivity and response of northern hemisphere altitudinal and polar treelines to environmental change at landscape and local scales: Treeline and environmental change. Glob Ecol Biogeography 14(5):395–410. https://doi.org/10.1111/j.1466- 822X.2005.00168.x

John B, Pandey HN, Tripathi RS (2001) Vertical distribution and seasonal changes of fine and coarse root mass in *Pinus kesiya* Royle Ex. Gordon forest of three different ages. Acta Oecologica 22:293–300. https://doi.org/10.1016/S1146-609X(01)01118-3

Karimi Z, Abdi E, Deljouei A, Cislaghi A, Shirvany A, Schwarz M, Hales TC (2022) Vegetation-induced soil stabilization in coastal area: An example from a natural mangrove forest. Catena, 216:106410. https://doi.org/10.1016/j.catena.2022.106410

Körner C (1999) Alpine plant life: Functional plant ecology of high mountain ecosystems. Springer.

Kramer JP, Boyer SJ (1995) Water Relations of Plants and Soils. Academic Press, San Diego, New York

Kumar P, Debele SE, Sahani J, Rawat N, Marti-Cardona B, Alfieri SM, Basu B, Basu AS, Bowyer P, Charizopoulos N, Gallotti G (2021) Nature-based solutions efficiency evaluation against natural hazards: Modelling methods, advantages and limitations. Science of the Total Environment 784:147058. https://doi.org/10.1016/j.scitotenv.2021.147058

Lin M, Sadeghi SMM, Van Stan JT (2020) Partitioning of rainfall and sprinkler-irrigation by crop canopies: A global review and evaluation of available research. Hydrology, 7(4):76. https://doi.org/10.3390/hydrology7040076

Loades KW, Bengough AG, Bransby MF, Hallett PD (2013) Biomechanics of nodal, seminal and lateral roots of barley: Effects of diameter, waterlogging and mechanical impedance. Plant Soil 370:407–418. https://doi.org/10.1007/s11104-013-1643-y

Loomis PF, Ruess RW, Sveinbjörnsson B, Kielland K (2006) Nitrogen cycling at treeline: latitudinal and elevational patterns across a boreal landscape. Ecoscience 13(4):544-556. https://doi.org/10.2980/1195-6860(2006)13[544:NCATLA]2.0.CO;2

Makarova OV, Cofie P, Koolen AJ (1998) Axial stress– strain relationships of fine roots of beech and larch in loading to failure and in cyclic loading. Soil Tillage Res 45:175–187. https://doi.org/10.1016/S0933-3630(97)00017-2

Mao Z, Saint-André L, Genet M, Mine FX, Jourdan C, Rey H, Courbaud B, Stokes A (2012) Engineering ecological protection against landslides in diverse mountain forests: Choosing cohesion models. Ecol Eng 45:55–69. https://doi.org/10.1016/j.ecoleng.2011.03.026

Mao Z (2022) Root reinforcement models: classification, criticism and perspectives. Plant Soil. https://doi.org/10.1007/s11104-021-05231-1

Mayor JR, Sanders, NJ, Classen AT, Bardget RD, Clément JC, Fajardo A, Lavorel S, Sundqvist MK, Bahn M, Chisholm C, Cieraad E, Gedalof Z, Grigulis K, Kudo G, Oberski DL, Wardle DA (2017) Elevation alters ecosystem properties across temperate treelines globally. Nature 542(7639):91–95. https://doi.org/10.1038/nature21027

Mazindrani, Z.H, Ganjali, MH (1997) Lateral earth pressure problem of cohesive backfill with inclined surface. Journal of Geotechnical and Geoenvironmental Engineering 123(2): 110–112.

McQueen DR (1968) The quantitative distribution of absorbing roots of *Pinus sylvestica* in a forest succession. Oecol. Plant 3:83–99

Mehtab A, Jiang YJ, Su LJ, Shamsher S, Li JJ, Mahfuzur R (2021) Scaling the Roots Mechanical Reinforcement in Plantation of Cunninghamia R. Br in Southwest China. Forests 12:33. https://doi.org/10.3390/f12010033

Milledge DG, Bellugi D, McKean JA, Densmore AL, Dietrich WE (2014) A multidimensional stability model for predicting shallow landslide size and shape across landscapes: predicting landslide size and shape. J. Geophys. Res. Earth Surf. 119:2481–2504. http://dx.doi.org/10.1002/2014JF003135

Montrasio L, Valentino R (2008) A model for triggering mechanisms of shallow landslides. Nat. Hazards Earth Syst Sci 8:1149–1159. https://doi.org/10.5194/nhess-8-1149-2008

Moore AM (1986) Temperature and moisture dependence of decomposition rates of hardwood and coniferous leaf litter. Soil Biol. Biochemis 18(4):427-435. https://doi.org/10.1016/0038-0717(86)90049-0

Moos C, Bebi P, Graf F, Mattli J, Rickli C, Schwarz M (2016) How does forest structure affect root reinforcement and susceptibility to shallow landslides?: A Case Study in St. Antönien, Switzerland. Earth Surf Process Landf 41:951–960. https://doi.org/10.1002/esp.3887

Moresi FV, Maesano M, Matteucci G, Romagnoli M, Sidle RC, Scarascia Mugnozza G (2019) Root biomechanical traits in a montane Mediterranean forest watershed: variations with species diversity and soil depth. Forests 10:341. https://doi.org/10.3390/f10040341

Morgan RP, Rickson RJ (1995) Slope stabilization and erosion control: a bioengineering approach. Second edition. Chapman and Hall, 293 p

Norris JE, Iorio AD, Stokes A, Nicoll BC, Achim A (2008) Species selection for soil reinforcement and protection. In Slope stability and erosion control: ecotechnological solutions. Springer, Dordrecht

O'Loughlin CL (1974) A study of tree root strength deterioration following clear felling. Canadian Journal of Forest Research 4:107–113. https://doi.org/10.1139/x74-016

Panahandeh T, Attarod P, Sadeghi SMM, Bayramzadeh V, Tang Q, Liu X (2022) The performance of the reformulated Gash rainfall interception model in the Hyrcanian temperate forests of northern Iran. Journal of Hydrology 612:128092. https://doi.org/10.1016/j.jhydrol.2022.128092

765 Phillips CJ, Marden M, Lambie S (2014) Observations of root growth of young poplar and willow planting types. N Z
766 J For Sci 44:15. https://doi.org/10.1186/s40490-014-0015-6

767 Pollen N, Simon A (2005) Estimating the mechanical effects of riparian vegetation on stream bank stability using a
768 fiber bundle model. Water Resour. Res. 41:W07025. https://doi.org/10.1029/2004WR003801

769 Pourghasemi H, Pradhan B, Gokceoglu C, Moezzi KD (2012) Landslide susceptibility mapping using a spatial multi
770 criteria evaluation model at Haraz Watershed, Iran. In: Pradhan B, Buchroithner M (eds) Terrigenous mass movements.
771 Springer, Berlin, pp. 23–49. https://doi.org/10.1007/978-3-642-25495-6_2

772 Rahbarisisakht S, Moayeri MH, Hayati E, Sadeghi SMM, Kepfer-Rojas S, Pahlavani MH, Kappel Schmidt I, Borz SA
773 (2021) Changes in soil's chemical and biochemical properties induced by road geometry in the Hyrcanian temperate
774 forests. Forests, 12:1805. https://doi.org/10.3390/ f12121805

775 Roering JJ, Schmidt KM, Stock JD, Dietrich WE, Montgomery DR (2003) Shallow landsliding, root reinforcement,
776 and the spatial distribution of trees in the Oregon Coast Range. Canadian Geotechnical J 40(2):237–253.
777 https://doi.org/10.1139/t02-113

778 Sadeghi SMM, Attarod P, Pypker TG (2015) Differences in rainfall interception during the growing and non-growing
779 seasons in a *Fraxinus rotundifolia* plantation located in a semiarid climate. J Agric Sci Technol 17:145–156

780 Sadeghi SMM, Gordon DA, Van Stan II JT (2020) A global synthesis of throughfall and stemflow hydrometeorology.
781 In Precipitation partitioning by vegetation (pp. 49-70). Springer, Cham. https://doi.org/10.1007/978-3-030-29702-2_4

782 Sagheb-Talebi K, Sajedi T, Pourhashemi M (2014) Euxino-Hyrcanian Province: Caspian and Arasbaran Regions. In:
783 Forests of Iran. Plant and Vegetation, vol 10. Springer, Dordrecht. https://doi.org/10.1007/978-94-007-7371-4_2

784 Schwarz M, Giadrossich F, Cohen D (2013) Modeling root reinforcement using a root-failureWeibull survival
785 function. Hydrol Earth Syst Sci 17:4367–4377. https://doi.org/10.5194/hess-17-4367-2013

786 Schwarz M, Lehmann P, Or D (2010) Quantifying lateral root reinforcement in steep slopes: from a bundle of roots to
787 tree stands. Earth Surf Process Landf 35:354–367. https://doi.org/10.1002/esp.1927

788 Schwarz M, Rist A, Cohen D, Giadrossich F, Egorov P, Buttner D, Stolz M, Thormann JJ (2015) Root reinforcement
789 of soils under compression. J. Geophys. Res. Earth Surf. 120:2103–2120. https://doi.org/10.1002/2015JF003632

790 See CR, McCormack LM, Hobbie SE., Flores-Moreno H, Silver WL, Kennedy PG (2019) Global patterns in fine root
791 decomposition: Climate, chemistry, mycorrhizal association and woodiness. Ecology Letters 22(6):946–953.
792 https://doi.org/10.1111/ele.13248

793 Sivandran G, Bras RL (2013) Dynamic root distributions in ecohydrological modeling: a case study at Walnut Gulch
794 Experimental Watershed. Water Resources Research 49:3292–3305. https://doi.org/10.1002/wrcr.20245

795 Stokes A, Norris JE, van Beck LPH, Bogaard T, Cammeraat E, Mickovski SB, Jenner A, Iorio AD, Fourcaud T (2008)
796 How vegetation reinforces the soil on slopes. Slope stability and erosion control: Ecotechnological solutions. Springer,
797 Dordrecht

798 Stokes A (2002) The biomechanics of tree root anchorage. Plant Roots, The Hidden Half, Plenum Publishing, New
799 York

800 Stokes A, Douglas GB, Fourcaud T, Giadrossich F, Gillies C, Hubble T, Kim JH, Loades KW, Mao Z, McIvor IR,
801 Mickovski SB (2014) Ecological mitigation of hillslope instability: ten key issues facing researchers and practitioners.
802 Plant Soil 377:1–23. https://doi.org/10.1007/s11104-014-2044-6

803 Sundqvist MK, Sanders NJ, Wardle DA (2013) Community and ecosystem responses to elevational gradients:
804 processes, mechanisms, and insights for global change. Ann Review Ecol Evol Systematics 44(1): 261-280.
805 https://doi.org/10.1146/annurev-ecolsys-110512-135750

806 Sveinbjörnsson B, Davis,J, Abadie W, Butler A (1995) Soil carbon and nitrogen mineralization at different elevations
807 in the Chugach Mountains of south-central Alaska, USA. Arctic Alpine Resear 27(1):29-37.
808 https://doi.org/10.2307/1552065

809 Taub DR, Goldberg D (1996) Root system topology of plants from habitats differing in soil resource availability. Funct
810 Ecol 258–264. https://doi.org/10.2307/2389851

811 Taylor DW (1948) Fundamentals of soil mechanics. Soil Sci. 66:161

812 Tsige D, Senadheera S, Talema A (2020) Stability analysis of plant-root-reinforced shallow slopes along mountainous
813 road corridors based on numerical modeling. Geosciences 10:19. https://doi.org/10.3390/geosciences10010019

814 Vergani C, Chiaradia EA, Bischetti GB (2012) Variability in the tensile resistance of roots in Alpine forest tree species.
815 Ecol Eng 46:43–56. https://doi.org/10.1016/j.ecoleng.2012.04.036

816 Vergani C, Giadrossich F, Buckley P, Conedera M, Pividori M, Salbitano F, Rauch HP, Lovreglio R, Schwarz M
817 (2017a) Root reinforcement dynamics of European coppice woodlands and their effect on shallow landslides: A
818 review. Earth Sci Rev 167:88–102. https://doi.org/10.1016/j.earscirev.2017.02.002

819 Vergani C, Werlen M, Conedera M, Cohen D, Schwarz M (2017b) Investigation of root reinforcement decay after a
820 forest fire in a Scots pine (*Pinus sylvestris*) protection forest. Forest Ecology and Management 400:339–352.
821 https://doi.org/10.1016/j.foreco.2017.06.005

822 Vergani C, Schwarz M, Cohen D, Thormann JJ, Bischetti GB (2014) Effects of root tensile force and diameter
823 distribution variability on root reinforcement in the Swiss and Italian Alps. Can J For Res 44:1426–1440.
824 https://doi.org/10.1139/cjfr-2014-0095

825 Waldron LJ (1977) The shear resistance of root-permeated homogeneous and stratified soil. Soil Sci. Soc. America J.
826 41:843–849.

827 Weemstra M, Freschet GT, Stokes A, Roumet C (2021) Patterns in intraspecific variation in root traits are species-
828 specific along an elevation gradient. Functional Ecol 35(2):342-356. https://doi.org/10.1111/1365-2435.13723

829 Wilkinson PL, Anderson MG, Lloyd DM, Renaud JP (2002) Landslide hazard and bioengineering: towards providing
830 improved decision support through integrated numerical model development. Environ Model Softw 17:333–344.
831 https://doi.org/10.1016/S1364-8152(01)00078-0

832 Williams CJ, Pierson FB, Kormos PR, Al-Hamdan OZ, Johnson JC (2020) Vegetation, ground cover, soil, rainfall
833 simulation, and overland-flow experiments before and after tree removal in woodland-encroached sagebrush steppe:
834 the hydrology component of the Sagebrush Steppe Treatment Evaluation Project (SageSTEP). Earth System Science
835 Data, 12(2):1347-1365. https://doi.org/10.5194/essd-12-1347-2020

836 Wu TH (1976) Investigation on landslides on Prince of Wales Island, Alaska. Geotech Rpt. No 5, Dpt. of Civil
837 Engineering, Ohio State University, Columbus, USA.

838 Yamase K, Todo C, Torii N, Tanikawa T, Yamamoto T, Ikeno H, Ohashi M, Dannoura M, Hirano, Y (2021) Dynamics
839 of soil reinforcement by roots in a regenerating coppice stand of *Quercus serrata* and effects on slope stability. Ecol
840 Eng 162:106169. https://doi.org/10.1016/j.ecoleng.2021.106169

841 Zhang C, Chen L, Jiang J, Zhou S (2012) Effects of gauge length and strain rate on the tensile strength of tree roots.
842 Trees 26:1577–1584. https://doi.org/10.1007/s00468-012-0732-5

843 Zydroń TA, Gruchot A (2021) Influence of root systems of deciduous trees on soil reinforcement. A case study from
844 the Carpathians, Poland. Environ Eng Manag J 20. https://doi.org/10.30638/eemj.2021.042

845 Zydroń TA, Gruchot A, Kluba M (2019) Spatial Variability of Reinforcement Provided by Juvenile Root Systems of
846 Black Locust and Black Poplar. Pol J Environ Stud 28:4027–4037. https://doi.org/10.15244/pjoes/96260

847 **Statements & Declarations**

848 **Funding**

849 The authors declare that no funds, grants, or other supports were received during the preparation of this manuscript.

850 **Competing Interests**

851 The authors have no competing interests to declare that are relevant to the content of this article.

852 **Author Contributions**

853 **Conceptualization:** Azade Deljouei, Alessio Cislaghi, Ehsan Abdi; **Methodology:** Azade Deljouei, Alessio Cislaghi;
854 **Formal analysis and investigation:** Azade Deljouei, Alessio Cislaghi; **Writing - original draft preparation:** Azade
855 Deljouei, Alessio Cislaghi; **Writing - review and editing:** Ehsan Abdi, Stelian Alexandru Borz, Baris Majnounian,
856 Tristram C. Hales; **Resources:** Azade Deljouei, Ehsan Abdi; **Supervision:** Ehsan Abdi, Baris Majnounian